The HITRAN database: 1986 edition

L. S. Rothman, R. R. Gamache, A. Goldman, L. R. Brown, R. A. Toth, H. M. Pickett, R. L. Poynter, J.-M. Flaud, C. Camy-Peyret, A. Barbe, N. Husson, C. P. Rinsland, and M. A. H. Smith

A description and summary of the latest edition of the AFGL HITRAN molecular absorption parameters database are presented. This new database combines the information for the seven principal atmospheric absorbers and twenty-one additional molecular species previously contained on the AFGL atmospheric absorption line parameter compilation and on the trace gas compilation. In addition to updating the parameters on earlier editions of the compilation, new parameters have been added to this edition such as the self-broadened halfwidth, the temperature dependence of the air-broadened halfwidth, and the transition probability. The database contains 348043 entries between 0 and 17,900 cm^{-1}. A FORTRAN program is now furnished to allow rapid access to the molecular transitions and for the creation of customized output. A separate file of molecular cross sections of eleven heavy molecular species, applicable for qualitative simulation of transmission and emission in the atmosphere, has also been provided.

I. Introduction

The high-resolution transmission molecular absorption database (known under the acronym HITRAN) is a compilation of spectroscopic parameters from which a wide variety of computer simulation codes are able to calculate and predict the transmission and emission of radiation in the atmosphere. This database is a prominent and long running effort established by the Air Force at the Air Force Geophysics Laboratory (AFGL) in the late 1960s in response to the requirement of a detailed knowledge of infrared transmission properties of the atmosphere. With the advent of sensitive detectors, rapid computers, and higher resolution spectrometers, a large database representing the discrete molecular transitions that affect radiative propagation throughout the electromagnetic spectrum became a necessity. A wide range of applications for HITRAN has evolved including detection of trace and weakly absorbing features in the atmosphere, atmospheric modeling efforts, laser transmission studies, remote sensing, lidar, and a reference base for fundamental laboratory spectroscopic research. The HITRAN database has been periodically updated and enhanced since it first became generally available.[1–4] The most recent edition of the HITRAN database was made available in late 1986. This latest version now unites the data on twenty-eight molecular species with bands covering regions from the millimeter through visible portion of the spectrum. Originally the database contained for each molecular transition the following basic parameters: (1) resonant frequency; (2) line intensity; (3) air-broadened halfwidth; and (4) lower state energy (as well as unique quantum identifications). Additional parameters have recently been provided which permit new capabilities for remote sensing in the atmosphere and capabilities to deal with nonlocal thermodynamic equilibrium effects in the upper atmosphere. The overall structure of the database has been expanded to include files of cross-sectional data on heavy molecular species such as the chlorofluorocarbons (CFCs) and oxides of nitrogen which are not yet amenable to line-by-line representation. This has added to HITRAN the capability of qualitative detection of anthropogenic gases in the window regions of the infrared. Ongoing research efforts will gradually move some of these data to the main body of the database. The new file structure of HITRAN is shown in Fig. 1. New parameters have been added to the

L. S. Rothman is with U.S. Air Force Geophysics Laboratory, Optical Physics Division, Hanscom Air Force Base, Massachusetts 01731; R. R. Gamache is with University of Lowell, Center for Atmospheric Research, Lowell, Massachusetts 01854; A. Goldman is with University of Denver, Physics Department, Denver, Colorado 80208; J.-M. Flaud and C. Camy-Peyret are with P. & M. Curie University, Laboratory of Molecular & Atmospheric Physics, 75252 Paris, France; A. Barbe is with Rheims University, Faculty of Sciences, 51062 Rheims, France; N. Husson is with Ecole Polytechnique, Dynamic Meteorology Laboratory, 91128 Palaiseau, France; C. P. Rinsland and M. A. H. Smith are with NASA Langley Research Center, Hampton, Virginia 23665; the other authors are with Jet Propulsion Laboratory, Pasadena, California 91109.

Received 17 April 1987.

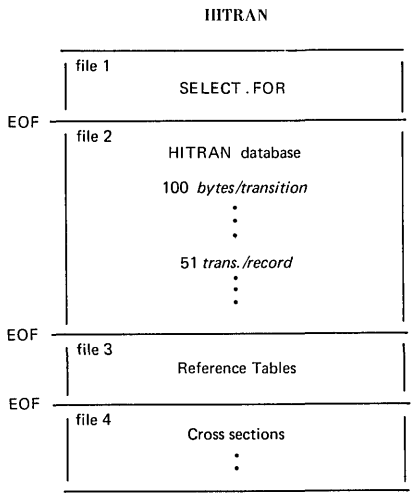

Fig. 1. File Structure of HITRAN.

present edition of HITRAN as well as fields included for anticipated parameters. Table I illustrates the actual image in the new database of an individual molecular transition. Formerly the database adhered to the card image concept, i.e., each transition was restricted to 80 characters; the new format has been expanded to 100 characters per transition. The new parameters are: the transition probability, the self-broadened halfwidth, and the exponent of temperature dependence of air-broadened halfwidth. Data fields have also been reserved for pressure shift of the transition, accuracy criteria for the three principal parameters, and references to the sources of the latter parameters. These fields have not at present been implemented (with some minor exceptions that will be discussed in Sec. II). We discuss below the definition of two of the newly presented parameters.

A parameter, R_{if}, which is both independent of temperature and isotopic abundance, has been added to the new edition of the database with the expectation that it will be quite useful for atmospheric calculations and applications utilizing Einstein coefficients. The transition probability, R_{if}, is related to the intensity of a transition, S_{if}, from state i to state f by

$$S_{if}(T) = \frac{8\pi^3}{3hc}\nu_{if}[1 - \exp(-c_2\nu_{if}/T)]\frac{g_i I_a}{Q(T)} \times \exp(-c_2 E_i/T)R_{if} \cdot 10^{-36}. \quad (1)$$

Here ν_{if} is the resonant frequency of the line, E_i is the energy of the lower state of the transition, g_i is the nuclear spin degeneracy of the lower level, $Q(T)$ is the total internal partition sum, I_a is the natural isotopic abundance, and c_2 is the second radiation constant (hc/k). The reference temperature T on the database is taken to be 296 K. The units for the parameters are given in Table I. In terms of the effective dipole matrix operator, M, R_{if} can be expressed as

$$R_{if} = |\langle i|\mathbf{M}|f\rangle|^2. \quad (2)$$

On the present compilation, R_{if} has been calculated as $R_{if}/Q(T_0)$. Thus a user, at this time, must multiply the current R_{if} value given on the compilation by the appropriate value of Q (296 K) to take full advantage of this parameter. In future editions Eq. (1), as well as the corresponding relation for quadrupole transitions,

$$S^q_{if}(T) = \frac{8\pi^5}{15hc}\nu^3_{if}[1 - \exp(-c_2\nu_{if}/T)]\frac{g_i I_a}{Q(T)} \times \exp(-c_2 E_i/T)R^q_{if} \cdot 10^{-36}, \quad (3)$$

will be fully implemented. Similar to the expression for intensities for dipolar transitions, R^q_{if} in Eq. (3) is expressed as the square of the matrix element of the quadrupole moment operator.

Provision for the self-broadened halfwidth, γ_s in cm^{-1}/atm at 296 K, has been made on the database. Presently, carbon dioxide and acetylene are the only two species where this parameter appears, although there is much available data for self-broadened halfwidths for other species; these will be introduced in subsequent editions of the database.

The exponent for temperature dependence of the air-broadened halfwidth has also been introduced in this edition. This parameter has begun to be measured accurately for various molecular species and has appeared in a previous edition of the GEISA (gestion et étude des informations spectroscopiques atmosphériques) databank.[5] The definition of the exponent, n, is given by

$$\gamma(T) = \gamma(T_0)\left(\frac{T_0}{T}\right)^n, \quad (4)$$

where $\gamma(T)$ is the air-broadened halfwidth in units of cm^{-1}/atm and T_0 is the reference temperature, 296 K. One should note the inversion of the temperature ratio in the definition in Eq. (4) which permits the storage of a positive value on the HITRAN database. Table II summarizes the range of values of the coefficient for each molecule presently in HITRAN.

A great amount of effort was also made for this edition to create a more uniform treatment of the rotational quantum numbers (and other quantum identifiers unique to a transition). Presently this has been accomplished by formatting the transitions into one of six classes, shown in Table III. In addition, the vibrational quantum numbers (and electronic designation where necessary) which cover whole bands have now been designated by indices to provide a rapid means of access for applications such as nonlocal thermodynamic equilibrium calculations. The isotopic variants of a species have also been assigned sequential indices in the order of the telluric relative abundance (see Table IV). For example, in Table I, molecule 2, i.e., CO_2, appears three times and the isotope code is 1, 2, or 3 corresponding, respectively, to 626($^{12}C^{16}O_2$), 636($^{13}C^{16}O_2$), and 628($^{16}O^{12}C^{18}O$). This has made it necessary to include correspondence tables in associated files on the database. The values of the natural isotopic abundance, I_a in Eqs. (3) and (4), assumed for the current HITRAN database are given in Table IV. In this version of the database, provision has also been made for the error estimates of the frequency, intensi-

Table I. Example of Direct Image of Lines on 1986 HITRAN Database

Mo	iso	Frequency ν	Intensity S	R	γ	γ_s	E"	n	δ or y	v'	v"	Q'	Q"	IER	IRef
31		800.276500	4.316E-25	3.777E-07	0.0599	0.0000	1162.00600	0.76	0.00000	2		12418 6	2517 9	382	0
281		800.287000	2.270E-23	4.717E-05	0.0750	0.0000	1483.94700	0.50	0.00000	2		117 7	18 7	381	0
101		800.301900	4.680E-23	2.421E-07	0.0630	0.0000	105.93600	0.50	0.00000	2		1 8 4 4	- 9 3 7	- 84	0
31		800.304700	1.286E-24	1.131E-05	0.0618	0.0000	1636.93510	0.76	0.00000	2		159 951	58 850	382	0
31		800.322500	1.243E-23	1.274E-06	0.0610	0.0000	720.65800	0.76	0.00000	2		11615 1	1614 2	382	0
101		800.322700	1.840E-22	2.195E-06	0.0630	0.0000	277.86000	0.50	0.00000	2		126 224	-25 125	- 84	0
23		800.326900	5.380E-26	2.668E-05	0.0793	0.1103	1326.41920	0.75	0.00000	8		3	R 13	186	0
271		800.332030	1.100E-22	3.212E-02	0.1000	0.0000	2354.24000	0.50	0.00000	19		14	4 8	382	0
101		800.361600	1.910E-22	2.278E-06	0.0630	0.0000	277.80700	0.50	0.00000	2		126 224	+25 125	+ 84	0
31		800.379600	6.830E-24	6.554E-07	0.0602	0.0000	707.21200	0.76	0.00000	2		11515 1	1514 2	382	0
101		800.416400	5.300E-23	1.025E-05	0.0630	0.0000	851.01800	0.50	0.00000	2		145 244	+44 143	+ 84	0
271		800.416750	1.330E-22	2.035E-02	0.1000	0.0000	2221.36110	0.50	0.00000	19		14	3 8	382	0
31		800.434100	4.723E-25	2.225E-05	0.0618	0.0000	1982.04700	0.76	0.00000	3		2501040	49 941	382	0
22		800.444000	6.390E-26	1.396E-04	0.0653	0.0846	1844.81880	0.75	0.00000	8		3	R 38	186	0
101		800.447000	5.180E-23	1.002E-05	0.0630	0.0000	851.04100	0.50	0.00000	2		145 244	-44 143	- 84	0
21		800.451200	3.210E-26	1.731E-05	0.0661	0.0872	2481.56150	0.75	0.00000	14		6	P 37	186	0

FORMAT (I2,I1,F12.6,1P2E10.3,0P2F5.4,F10.4,F4.2,F8.5,2I3,2A9,3I1,3I2)
- 100 characters per transition

This format corresponds as follows:

Mo - I2 - Molecule number
iso- I1 - Isotope number (1= most abundant, 2= second, etc.)
ν - F12.6 - Frequency in cm^{-1}
S - E10.3 - Intensity in $cm^{-1}/(molec \cdot cm^{-2})$ @ 296K
R - E10.3 - Transition probability in $Debyes^2$ (presently lacking internal partition sum)
γ - F5.4 - Air-broadened halfwidth (HWHM) in cm^{-1}/atm @ 296K
γ_s - F5.4 - Self-broadened halfwidth (HWHM) in cm^{-1}/atm @ 296K
E" - F10.4 - Lower state energy in cm^{-1}
n - F4.2 - Coefficient of temperature dependence of air-broadened halfwidth
y - F8.5 - Shift of transition due to pressure (presently empty; some coupling coefficients inserted)
v' - I3 - Upper state global quanta index
v" - I3 - Lower state global quanta index
Q' - A9 - Upper state local quanta
Q" - A9 - Lower state local quanta
IER- 3I1 - Accuracy indices for frequency†, intensity, and halfwidth
IRef-3I2 - Indices for lookup of references for frequency, intensity, and halfwidth (not presently used)

†IER code for frequency when used:

IER	estimated error in wavenumber
0	≥ 1.
1	≥ 0.1 and < 1.0
2	≥ 0.01 and < 0.1
3	≥ 0.001 and < 0.01
4	≥ 0.0001 and < 0.001
5	≥ 0.00001 and < 0.0001
6	< 0.00001

ty, and the air-broadened halfwidth (see Table I). This has only been implemented for some of the transitions as described in Sec. II.

The first file on the compilation is a FORTRAN program called SELECT that enables the user to interactively access the HITRAN database (the second file) to create files of portions of the atlas of interest based on selected criteria such as frequency range, molecule, isotope, vibrational bands, and intensity cutoff. The user can readily customize his output to correspond to specific program requirements or storage limitations.

Presently 348,043 transitions are given on the high resolution portion of HITRAN. A summary of the transitions now incorporated is given in Table V. The species are given in Table V in the order of their molecule index identification in the compilation. Figure 2 displays the spectral regions in which parameters can be found for each molecule in HITRAN.

In the following section modifications, updates, and additions to the database since the last edition[3,4] are discussed. This is not meant to be a definitive discussion, and users are advised to consult the references for more detailed information. As a convenience to the user, some of the major updates planned will also be mentioned.

II. New or Modified Data

A. H_2O

The ground state pure rotation band of the monodeuterated isotope of water (HDO) has been updated. The data are from the Jet Propulsion Laboratory (JPL) Catalog[6] and were derived from a fit which included the microwave and submillimeter lines reported by Messer *et al.*[7] and an extensive set of ground state energy levels from the high resolution FTS mea-

Table II. Range of Air-Broadened Halfwidths and Temperature Dependences

Molecule	γ min.	γ max.	n min.	n max.
H_2O	0.0061	0.1046	-- 0.64 --	
CO_2	0.0559	0.0899	0.75	0.79
O_3	0.045	0.077	-- 0.76 --	
N_2O	0.0686	0.0974	0.64	0.82
CO	0.047	0.088	-- 0.69 --	
CH_4	0.0445	0.0920	0.63	1.00
O_2	0.032	0.062	-- 0.5 ---	
NO	0.043	0.063	-- 0.5 ---	
SO_2	0.110	0.152	-- 0.5 ---	
NO_2	0.062	0.073	-- 0.5 ---	
NH_3	0.043	0.090	-- 0.5 ---	
HNO_3	-- 0.13 --		-- 0.5 ---	
OH	-- 0.083 --		-- 0.5 ---	
HF	0.020	0.126	-- 0.5 ---	
HCl	0.0135	0.0953	0.20	0.88
HBr	0.015	0.123	-- 0.5 ---	
HI	0.008	0.100	-- 0.5 ---	
ClO	-- 0.085 --		-- 0.5 ---	
OCS	-- 0.07 --		-- 0.5 ---	
H_2CO	0.107	0.108	-- 0.5 ---	
HOCl	-- 0.06 --		-- 0.5 ---	
N_2	-- 0.06 --		-- 0.5 ---	
HCN	0.0819	0.1566	-- 0.5 ---	
CH_3Cl	-- 0.08 --		-- 0.5 ---	
H_2O_2	-- 0.10 --		-- 0.5 ---	
C_2H_2	0.0400	0.1158	-- 0.75 --	
C_2H_6	-- 0.10 --		-- 0.5 ---	
PH_3	-- 0.075 --		-- 0.5 ---	

Table III. Formats of the Six Classes of Local Quanta

Group 1: Asymmetric Rotors,

H_2O, O_3, SO_2, NO_2, HNO_3, H_2CO, HOCl, H_2O_2, H_2S

J', K_a', K_c', F', Sym'; J", K_a", K_c", F", Sym"
I2, I2, I2, I2, A1 ; I2, I2, I2, I2, A1

Group 2: Diatomic and Linear Molecules with Integer J

CO_2, N_2O, CO, HF, HCl, HBr, HI, OCS, N_2, HCN, C_2H_2

____Br, F", _; ____Br, J", Sym"
5X,A1, I2,1X; 4X,A1, I3, A1

Group 3: Spherical Rotors

Methane (CH_4 only, not CH_3D)

J', R', C', N', Sym'; J", R", C", N", Sym"
I2, I2, A2, I2, A1 ; I2, I2, A2, I2, A1

Group 4: Symmetric Rotors

CH_3D, NH_3, CH_3Cl, C_2H_6*, PH_3

J', K', C', __, Sym'; J", K", C", __, Sym"
I2, I2, A2, 2X, A1 ; I2, I2, A2, 2X, A1

Group 5: Triplet Ground Electronic States

O_2

___Br, F" , _; Br, N", Br, J", __, Sym"
3X,A1, F4.1, 1X; A1, I2, A1, I2, 2X, A1

Group 6: Doublet Ground Electronic States (Half Integer J)

NO, OH, ClO

_____, Br, F" , _; ___, Br, J" , Sym"
5X, A1, I2, 1X; 3X, A1, F4.1, A1

Notes: Prime and double primes refer to upper and lower states respectively; Br is the P-, Q-, or R- branch symbol; J is the rotational quantum number; Sym is e or f for l-type doubling, + or - for symmetry, etc. (for further explanation see references).

* presently using group 2 quantum notation on the tape.

surements of Toth.[8] The estimated uncertainty of the line positions varies from line to line and ranges from 0.02 to 0.000001 cm^{-1} for these lines. The uncertainty is given for each line in the parameter IER(1) on the HITRAN database (see Table I). The line intensities are accurate to 2–5%.

The bands of water in the 6.3- and 2.7-μm regions shown in Table V have been updated by incorporating

Table IV. Isotopic Variants in HITRAN

Molecule	AFGL isotope code	relative natural abundance	Molecule	AFGL isotope code	relative natural abundance
H_2O	161	0.9973	HNO_3	146	0.9891
	181	0.0020			
	171	0.0004	OH	61	0.9975
	162	0.0003		81	0.0020
				62	0.00015
CO_2	626	0.9842			
	636	0.0110	HF	19	0.99985
	628	0.0039			
	627	0.0008	HCl	15	0.7576
	638	0.000044		17	0.2423
	637	0.000009			
	828	0.0000040	HBr	19	0.5068
	728	0.000002		11	0.4930
O_3	666	0.9928	HI	17	0.99985
	668	0.0040			
	686	0.0020	ClO	56	0.7559
				76	0.2417
N_2O	446	0.9904			
	456	0.0036	OCS	622	0.937
	546	0.0036		624	0.0416
	448	0.0020		632	0.0105
	447	0.0004		822	0.0019
CO	26	0.9865	H_2CO	126	0.9862
	36	0.011		136	0.0111
	28	0.0020		128	0.0020
	27	0.0004			
			HOCl	165	0.7558
CH_4	211	0.9883		167	0.2417
	311	0.0111			
	212	0.00059	N_2	44	0.9928
O_2	66	0.9952	HCN	124	0.9852
	68	0.0040		134	0.0111
	67	0.0008		125	0.0036
NO	46	0.9940	CH_3Cl	215	0.7490
	56	0.0036		217	0.2395
	48	0.0020			
			H_2O_2	1661	0.9949
SO_2	626	0.9454			
	646	0.0420	C_2H_2	1221	0.9776
				1231	0.0219
NO_2	646	0.9916			
			C_2H_6	1221	0.9776
NH_3	4111	0.9960			
	5111	0.0036	PH_3	1111	0.99955

data from Flaud *et al.*[9] These are the bands that were not previously[3] added to the database from Ref. 9. With the addition of the data in Table V, all the data of Flaud *et al.*[9] are present on the database producing a self-consistent set of water data. In general the accuracy of the line positions is better than ±0.005 cm^{-1}, and the line intensities are accurate to ≈20% (with the weaker lines being somewhat less accurate). The data show a deterioration of accuracy for high J lines.[10]

The ν_2 band of monodeuterated water has been replaced with the data of Toth.[8] The line positions are accurate to ±0.0004 cm^{-1} for all unblended lines and slightly blended lines of medium to strong intensity. The line intensities were calculated by the F-factor formalism with corrections for centrifugal distortion and the $\Delta\kappa$ effect. The line intensities are accurate to ~5% for the stronger lines and for the weaker lines the uncertainty is ≈20%.

The air-broadened halfwidths of all water vapor lines on the database have been updated using the calculations of Gamache and Davies[11] for the principal isotopic species ($H_2{}^{16}O$) and the optimum combination algorithm[12,13] for all other species (HDO, $H_2{}^{17}O$, $H_2{}^{18}O$). All calculations were for N_2 broadening and have been scaled to air using the factor 0.9. Values for the principal isotope have an estimated uncertainty

Table V. Band Centers and Band Sums

Band Centers	Isotope	Vibrational Band upper	lower	Frequency min	max	number lines	Sum of Intensity	
	H_2O Molecule: number of lines = 47202							
	161	000-	000	0-	1648	1728	5.268E-17	N
	181	000-	000	6-	977	766	1.066E-19	
	171	000-	000	6-	906	622	1.943E-20	
	162	000-	000	0-	101	461	2.585E-21	N
	161	010-	010	0-	1030	750	2.225E-20	
	181	010-	010	21-	559	202	4.632E-23	
	171	010-	010	21-	449	117	7.921E-24	
	161	020-	020	26-	503	129	1.016E-23	
	161	100-	100	86-	302	27	5.977E-25	
	161	001-	001	86-	292	19	3.072E-25	
1403.489	162	010-	000	1104-	1895	1653	2.816E-21	N
1515.163	161	030-	020	1271-	1932	121	5.135E-24	
1550.774	181	020-	010	1287-	1960	187	1.644E-23	
1553.653	171	020-	010	1343-	1860	86	2.464E-24	
1556.883	161	020-	010	995-	2407	686	8.157E-21	N
1588.279	181	010-	000	1009-	2220	852	2.101E-20	N
1591.325	171	010-	000	1063-	2156	668	3.823E-21	
1594.7498	161	010-	000	782-	2910	1741	1.038E-17	N
2062.306	161	100-	010	1221-	2520	402	1.820E-22	N
2153.288	181	001-	010	2066-	2267	16	2.267E-25	
2161.183	161	001-	010	1298-	2612	365	2.626E-22	N
2723.6799	162	100-	000	2332-	3133	1333	6.337E-22	
2782.0117	162	020-	000	2486-	3362	953	8.468E-23	
3072.046	161	030-	010	2813-	3917	313	7.303E-23	
3139.053	181	020-	000	2806-	4046	388	1.325E-22	
3144.978	171	020-	000	2887-	3994	247	2.409E-23	
3151.630	161	020-	000	2565-	4339	1132	7.571E-20	N
3632.961	181	110-	010	3624-	3790	3	7.920E-26	
3640.245	161	110-	010	3172-	4145	365	1.946E-22	
3649.685	181	100-	000	3108-	4194	553	9.468E-22	
3653.143	171	100-	000	3223-	4127	387	1.699E-22	
3657.053	161	100-	000	2823-	4347	1302	4.955E-19	N
3707.467	162	001-	000	3236-	4122	1651	1.416E-21	
3719.891	161	021-	020	3570-	3869	49	1.158E-24	
3722.189	181	011-	010	3525-	3912	101	5.356E-24	
3728.937	171	011-	010	3591-	3858	34	6.618E-25	
3736.522	161	011-	010	3203-	4282	527	2.923E-21	
3741.567	181	001-	000	3160-	4341	711	1.393E-20	
3748.318	171	001-	000	3227-	4243	529	2.516E-21	
3755.930	161	001-	000	2894-	4350	1546	7.200E-18	N

continued

from 10 to 15%, with the less abundant species being slightly less accurate (20%).

B. CO_2

A complete update of the energy levels and intensities of the carbon dioxide parameters has been implemented for this edition of HITRAN. A summary of this effort is given by Rothman[14] which has been enhanced by the great amount of high resolution line positions of many bands observed in the period since the last edition of the database. More importantly, in this period Fourier transform spectrometers and diode laser systems have provided measurements of many band and line intensities of unprecedented photometric accuracy. The theoretical technique of Wattson and Rothman[15] has also been applied so that a higher-

Table V, continuation 1

4099.956	162	110-	000	3843-	4497	860	6.426E-23
4145.473	162	030-	000	3879-	4640	602	3.504E-23
4666.793	161	030-	000	4250-	5932	662	3.955E-22
5089.539	162	011-	000	4850-	5385	576	3.671E-23
5221.24	181	110-	000	4791-	5728	443	5.646E-23
5234.977	161	110-	000	4602-	6006	991	3.716E-20
5276.776	161	021-	010	4908-	5812	285	6.620E-22
5310.468	181	011-	000	4808-	5963	734	1.476E-21
5320.262	171	011-	000	5505-	5840	86	9.627E-24
5331.269	161	011-	000	4609-	6255	1306	8.042E-19
5372.114	162	200-	000	5154-	5508	216	1.589E-23
6134.030	161	040-	000	5904-	7190	215	1.785E-23
6775.10	161	120-	000	6227-	7522	610	3.047E-21
6871.51	161	021-	000	6205-	7804	930	5.061E-20
7201.54	161	200-	000	6446-	7940	976	4.579E-20
7249.811	161	101-	000	6489-	8051	1361	6.431E-19
7445.07	161	002-	000	6832-	8183	813	5.837E-21
8238.84	161	041-	010	8083-	8506	77	1.207E-24
8273.95	161	130-	000	7845-	8984	328	2.329E-22
8341.32	181	031-	000	8181-	8656	102	1.627E-24
8356.70	171	031-	000	8240-	8533	35	1.913E-25
8373.82	161	031-	000	7948-	9127	429	8.939E-22
8734.97	161	121-	010	7759-	9089	247	3.990E-23
8761.579	161	210-	000	8198-	9207	378	4.151E-22
8779.75	181	111-	000	8472-	9192	335	9.856E-23
8792.63	171	111-	000	8538-	9072	226	1.807E-23
8807.000	161	111-	000	8188-	9556	833	4.946E-20
8966.53	181	012-	000	8722-	9291	155	2.873E-24
8983.	171	012-	000	8808-	9241	58	3.803E-25
9000.13	161	012-	000	8569-	9671	511	1.557E-21
9833.58	161	041-	000	9607-	10381	153	4.269E-23
10284.4	161	220-	000	10050-	10568	112	1.002E-23
10298.	181	121-	000	9412-	10545	141	3.970E-24
10314.	171	121-	000	10158-	10505	70	6.360E-25
10328.72	161	121-	000	9276-	11027	478	2.083E-21
10524.3	161	022-	000	10293-	10800	99	4.099E-24
10581.	181	201-	000	10285-	10905	279	4.202E-23
10597.	171	201-	000	10344-	10823	175	7.641E-24
10599.66	161	300-	000	10143-	11028	357	2.585E-22
10613.41	161	201-	000	9999-	11183	782	2.116E-20
10868.86	161	102-	000	9364-	11300	389	5.649E-22
10990.	181	003-	000	10761-	11164	147	4.560E-24
11011.	171	003-	000	10855-	11151	76	7.311E-25
11032.	161	003-	000	10507-	11529	559	2.381E-21
11813.19	161	131-	000	11522-	12373	220	5.362E-23
12139.2	161	310-	000	11808-	12456	221	1.317E-23
12151.26	161	211-	000	11689-	12697	458	9.284E-22
12407.64	161	112-	000	12055-	12753	212	2.575E-23
12565.00	161	013-	000	12249-	12938	240	8.417E-23

continued

Table V, continuation 2

13256.	161	141-	000	13291- 13829	41	2.557E-24
13448.	161	042-	000	13319- 13942	8	1.433E-24
13642.	161	320-	000	13480- 13940	16	6.094E-24
13652.65	161	221-	000	13311- 14163	216	1.767E-22
13820.922	161	301-	000	13274- 14217	330	1.083E-21
13828.3	161	202-	000	13318- 14143	169	7.894E-23
13910.8	161	122-	000	13549- 14138	38	3.216E-24
14066.193	161	023-	000	13932- 14425	63	6.970E-24
14221.143	161	400-	000	13958- 14647	173	3.975E-23
14318.802	161	103-	000	13926- 14657	235	2.052E-22
14536.87	161	004-	000	14137- 14776	64	2.423E-24
14640.	161	151-	000	14922- 15220	2	4.602E-26
15107.	161	330-	000	15250- 15415	2	1.764E-25
15119.026	161	231-	000	14907- 15525	106	4.649E-24
15344.499	161	212-	000	15083- 15667	110	1.379E-23
15347.949	161	311-	000	14945- 15724	237	8.775E-23
15742.787	161	410-	000	15606- 15939	35	9.991E-25
15832.757	161	113-	000	15584- 15965	109	1.200E-23
16821.626	161	321-	000	16465- 17192	143	4.351E-23
16825.23	161	222-	000	16624- 17108	48	5.582E-24
16898.4	161	302-	000	16487- 17092	134	2.096E-23
16898.828	161	401-	000	16486- 17228	227	8.554E-23
17227.7	161	420-	000	17129- 17281	10	1.104E-25
17312.54	161	123-	000	17125- 17628	77	1.819E-24
17458.203	161	500-	000	17145- 17715	108	3.945E-24
17495.517	161	203-	000	17143- 17787	182	1.839E-23
17748.073	161	104-	000	17473- 17880	49	2.499E-25

continued

order self-consistent set of band intensities for the parallel bands of the main isotope have been furnished. The extensive new high resolution observations provide access to the majority of the vibrational energy levels for the two most abundant isotopic species below ~7000 cm^{-1}. For the most abundant asymmetric species, $^{12}C^{16}O^{18}O$, this is also true up to ~5000 cm^{-1}.

Of the 634 bands of carbon dioxide considered, 573 survived the intensity criterion to be included on the HITRAN database. Line positions that have been interpolated from the least-squares fit of observed transitions[14] are generally accurate to 0.0004 cm^{-1}. Some line positions have accuracies good to 0.0001 cm^{-1}; however, due to the calibration problem discovered between different spectroscopic facilities,[16] there remains a discrepancy of the former amount in many cases (see additional discussion of this problem below under the subsection for the methane molecule). This absolute calibration problem will be addressed in future work on the line positions. The intensities that have been updated are believed to be good to ~10%. Much work is in progress at this time to improve the intensities of the bands on the database. Observations are being made on significant perpendicular bands previously only approximated, and important results are being obtained to provide higher-order reliable Herman-Wallis coefficients which will greatly improve the accuracy of the higher rotational lines than is now on the database.

New air-broadened halfwidths have been applied to all the carbon dioxide lines on the database. These have been taken from Arié *et al.*[17] A linear regression fit was applied to their data to extend the air-broadened values from $|m| = 40$ to 80; a constant value of 0.0606 cm^{-1}/atm was assumed beyond $|m| = 80$. (The running index m equals $-J''$ for the P branch, J'' for the Q branch, and $J'' + 1$ for the R branch.) The new values of halfwidth generally parallel the previous results, but show higher values at low J. These new parameters have been assumed for all bands and isotopes. Similarly, self-broadened halfwidths have been taken from Ref. 17 and have been adopted for all CO_2 bands.

Sizable discrepancies have been observed for some time between observed and simulated spectra using the normal set of molecular parameters in the vicinity of strong Q branches.[18] This difference has been especially noted in the 15-μm region of CO_2. This phenomenon is attributed to line coupling (also called rotational collisional narrowing, line mixing, line interference, or Q-branch collapse) which manifests itself as a distortion of the line shape. For this edition, line coupling coefficients for three perpendicular bands, the

Table V, continuation 3

CO_2 molecule: number of lines = 59554
Number of bands on Compilation = 573

Band Centers	Vibrational band upper	lower	Isotope	Frequency min - max	Intensity (x10 ^{22})	number lines
471.511	20003	11101	626	444 - 502	0.00740	56
479.898	13302	12201	626	479 - 481	0.00041	25
494.586	12202	11101	636	494 - 496	0.00021	17
508.167	12202	11101	626	474 - 548	0.04681	135
510.320	21103	20002	626	489 - 536	0.00310	42
526.475	11102	10001	636	493 - 568	0.03212	73
535.893	11102	10001	628	512 - 563	0.00916	99
542.220	21102	20001	626	514 - 571	0.00615	53
544.286	11102	10001	626	493 - 600	2.53368	104
557.608	14402	05501	626	546 - 558	0.00088	22
561.121	12202	03301	628	560 - 562	0.00152	34
564.909	20002	11101	628	563 - 565	0.00160	27
568.906	13302	04401	626	530 - 606	0.06614	136
573.451	13302	04401	636	573 - 574	0.00039	24
576.596	11102	02201	628	537 - 614	0.15718	300
578.631	21102	12201	626	543 - 613	0.03460	130
579.141	20002	11101	627	578 - 579	0.00018	16
581.361	22203	13302	626	555 - 607	0.00803	89
581.776	12202	03301	626	529 - 631	1.80860	189
585.328	12202	03301	636	551 - 619	0.03123	124
586.852	11102	02201	627	554 - 618	0.03985	240
594.288	20002	11101	626	541 - 641	0.85612	97
595.601	21103	12202	636	582 - 597	0.00162	31
596.441	21103	12202	626	551 - 642	0.24187	164
597.052	10002	01101	628	542 - 647	4.89982	213
597.338	11102	02201	626	532 - 658	49.14497	229
599.023	20003	11102	628	598 - 599	0.00095	20
599.274	11102	02201	636	551 - 648	0.66245	179
601.571	10002	01101	638	567 - 637	0.05136	144
607.554	20003	11102	627	590 - 627	0.00368	74
607.558	10002	01101	627	559 - 655	1.10759	191
607.968	20002	11101	636	577 - 639	0.01015	61
608.830	10012	01111	626	576 - 642	0.01626	66
609.586	10002	01101	637	584 - 637	0.00902	98
610.989	20003	11102	636	571 - 655	0.09648	82
615.897	20003	11102	626	561 - 674	6.54097	109
617.350	10002	01101	636	560 - 678	19.47982	115
618.029	10002	01101	626	546 - 686	1364.29129	136
619.753	21103	20003	636	591 - 651	0.00770	57
630.710	11102	10002	636	578 - 685	2.48321	104
633.097	21103	20003	626	584 - 683	0.62014	95
636.751	01111	00011	636	607 - 670	0.01126	63
637.531	13302	12202	636	612 - 669	0.01166	101
642.311	11102	10002	628	599 - 691	0.74667	188
643.329	01101	00001	638	595 - 697	3.41927	209
643.653	02201	01101	638	606 - 687	0.28668	320
644.408	11102	10002	627	606 - 687	0.14319	161
645.744	01101	00001	637	602 - 694	0.61476	182
646.083	02201	01101	637	616 - 682	0.05126	247
647.062	11102	10002	626	583 - 716	212.88226	128
647.712	12202	11102	628	617 - 684	0.05625	259
648.478	01101	00001	636	582 - 721	824.74876	134

continued

Table V, continuation 4

648.786	02201 - 01101	636	590 - 718	70.50468	235
649.087	03301 - 02201	636	599 - 707	4.51143	200
649.408	04401 - 03301	636	609 - 697	0.25569	159
649.435	05501 - 04401	636	625 - 682	0.01280	94
649.953	12202 - 11102	627	633 - 673	0.00850	134
652.552	12202 - 11102	626	597 - 717	15.86638	217
654.869	01111 - 00011	626	607 - 707	0.84957	97
655.261	02211 - 01111	626	619 - 696	0.07251	145
655.601	13302 - 12202	626	611 - 708	0.95297	180
657.331	01101 - 00001	828	615 - 703	0.32923	96
657.704	14402 - 13302	626	625 - 697	0.04204	128
657.753	02201 - 01101	828	629 - 691	0.02586	129
659.706	01101 - 00001	728	626 - 697	0.06042	150
661.136	13301 - 12201	636	661 - 685	0.00378	56
662.374	01101 - 00001	628	603 - 730	317.39860	259
662.768	02201 - 01101	628	611 - 724	25.23559	442
663.171	12201 - 11101	636	626 - 707	0.10161	151
663.187	03301 - 02201	628	620 - 713	1.44563	364
663.603	04401 - 03301	628	633 - 700	0.07391	254
664.729	01101 - 00001	627	608 - 729	59.85706	238
665.114	02201 - 01101	627	617 - 721	4.70133	396
665.509	03301 - 02201	627	628 - 709	0.27389	308
667.031	11101 - 10001	636	617 - 721	1.52147	101
667.380	01101 - 00001	626	593 - 752	79451.72586	153
667.752	02201 - 01101	626	599 - 750	6257.19909	276
668.115	03301 - 02201	626	608 - 740	368.83823	247
668.213	21102 - 20002	626	624 - 718	0.30043	91
668.471	04401 - 03301	626	615 - 732	19.33590	214
669.002	05501 - 04401	626	624 - 722	0.94472	174
669.350	06601 - 05501	626	634 - 712	0.07408	132
678.998	12201 - 11101	628	648 - 715	0.05659	259
680.053	14401 - 13301	626	651 - 715	0.02345	113
681.386	12201 - 11101	627	681 - 700	0.00510	114
681.491	13301 - 12201	626	638 - 731	0.44473	170
683.495	11101 - 10001	628	638 - 731	0.74282	188
683.869	12201 - 11101	626	630 - 746	8.75200	211
686.071	11101 - 10001	627	647 - 727	0.12500	158
688.671	11101 - 10001	626	625 - 755	144.01364	125
696.689	22201 - 21101	626	668 - 730	0.01810	114
698.949	10001 - 01101	638	663 - 734	0.05542	147
703.470	10001 - 01101	628	650 - 758	7.92937	219
703.536	21101 - 20001	626	658 - 749	0.23806	88
707.839	20001 - 11101	628	678 - 740	0.02249	127
709.373	10001 - 01101	637	684 - 734	0.00806	95
710.771	10011 - 01111	626	675 - 745	0.01923	68
711.299	10001 - 01101	627	662 - 759	1.21906	192
712.511	20002 - 11102	628	685 - 739	0.01162	107
713.496	20001 - 11101	627	712 - 714	0.00141	25
713.503	20001 - 11101	636	674 - 752	0.04522	76
720.280	20001 - 11101	626	668 - 779	4.63994	107
720.805	10001 - 01101	626	649 - 789	1395.61260	136
721.584	10001 - 01101	636	658 - 777	17.05190	115
724.198	11101 - 02201	628	682 - 764	0.30406	320
724.545	20002 - 11102	627	721 - 725	0.00109	37
732.256	11101 - 02201	627	699 - 764	0.04445	242
733.508	21101 - 12201	636	731 - 734	0.00093	35
738.673	20002 - 11102	626	679 - 788	2.93417	105

continued

Table V, continuation 5

739.829	11101 - 02201	636	689 - 785	0.67911	179
739.948	21101 - 12201	626	696 - 783	0.17040	159
740.009	12201 - 03301	628	715 - 762	0.01313	170
741.724	11101 - 02201	626	673 - 803	76.72998	235
748.133	12201 - 03301	627	747 - 749	0.00096	54
748.524	20002 - 11102	636	709 - 784	0.03646	74
754.334	21102 - 12202	626	708 - 794	0.15602	157
757.479	12201 - 03301	626	702 - 807	3.19758	195
765.641	13301 - 04401	636	764 - 766	0.00071	31
770.498	13301 - 04401	626	727 - 809	0.13085	149
771.266	11101 - 10002	636	726 - 812	0.13458	84
781.550	14401 - 05501	626	758 - 782	0.00358	51
789.812	11101 - 10002	627	765 - 817	0.00876	97
789.913	11101 - 10002	628	756 - 828	0.05430	147
790.989	21102 - 20003	626	749 - 829	0.05338	78
791.447	11101 - 10002	626	735 - 849	8.66292	110
803.727	12201 - 11102	636	788 - 825	0.00351	57
828.255	12201 - 11102	626	788 - 873	0.14810	156
829.529	21101 - 20002	626	801 - 863	0.01093	61
857.193	13301 - 12202	626	833 - 886	0.00988	93
864.666	20001 - 11102	626	827 - 904	0.04107	75
883.145	01111 - 11101	636	853 - 909	0.00533	64
898.548	02211 - 12201	626	861 - 927	0.01380	84
913.425	00011 - 10001	636	864 - 950	0.07587	56
915.650	21101 - 12202	626	913 - 916	0.00087	34
917.647	10011 - 20001	626	878 - 946	0.00965	44
927.156	01111 - 11101	626	868 - 965	0.41439	139
941.698	10012 - 20002	626	901 - 974	0.01356	47
952.306	21101 - 20003	626	952 - 954	0.00027	15
960.959	00011 - 10001	626	886 -1002	6.80082	75
963.986	00011 - 10001	627	937 - 986	0.00366	56
966.269	00011 - 10001	628	927 - 994	0.01732	88
1017.659	00011 - 10002	636	965 -1050	0.05342	55
1023.701	01111 - 11102	636	988 -1049	0.00847	73
1043.640	10011 - 20002	626	1002 -1075	0.01568	47
1063.735	00011 - 10002	626	986 -1105	9.68632	77
1064.475	10012 - 20003	626	1016 -1095	0.03197	51
1066.242	11112 - 21103	626	1042 -1086	0.00217	43
1067.727	00011 - 10002	627	1037 -1092	0.00567	66
1071.542	01111 - 11102	626	1010 -1109	0.76264	149
1072.687	00011 - 10002	628	1030 -1103	0.03537	99
1074.250	02211 - 12202	626	1031 -1105	0.03038	98
1239.363	11102 - 01101	628	1209 -1271	0.02088	156
1244.900	10002 - 00001	638	1228 -1266	0.00152	34
1259.426	10002 - 00001	628	1214 -1305	0.31915	123
1272.287	10002 - 00001	627	1239 -1305	0.01462	84
1342.278	10001 - 00001	638	1316 -1370	0.00553	66
1365.844	10001 - 00001	628	1322 -1414	0.35848	124
1376.027	10001 - 00001	627	1342 -1412	0.02164	91
1386.965	11101 - 01101	628	1354 -1421	0.03300	176
1846.332	21103 - 02201	626	1807 -1882	0.00731	69
1859.049	20003 - 01101	636	1832 -1847	0.00046	10
1880.987	20003 - 01101	626	1830 -1934	0.11931	86
1883.201	12202 - 01101	636	1856 -1873	0.00120	23
1889.514	22203 - 11102	626	1860 -1879	0.00149	26

continued

Table V, continuation 6

1896.055	21103 - 10002	626	1852	-1941	0.02052	69
1896.538	11102 - 00001	636	1852	-1944	0.03902	78
1901.737	11102 - 00001	628	1860	-1937	0.03060	124
1905.491	13302 - 02201	626	1866	-1946	0.01805	113
1916.695	11102 - 00001	627	1884	-1918	0.00434	59
1917.642	12202 - 01101	626	1867	-1975	0.37932	186
1932.470	11102 - 00001	626	1871	-1999	6.22904	117
1951.171	21102 - 10001	626	1910	-1959	0.01076	50
1996.583	20002 - 01101	636	1957	-1997	0.00413	38
2003.246	03301 - 00001	626	1955	-2074	0.00226	87
2003.763	20002 - 01101	626	1954	-2042	0.03110	71
2004.224	21102 - 02201	626	1979	-2005	0.00139	31
2023.870	21102 - 10002	636	1994	-2015	0.00072	13
2037.093	11101 - 00001	636	1980	-2089	0.62952	100
2049.339	11101 - 00001	628	2003	-2086	0.17540	152
2051.786	12201 - 01101	636	2006	-2091	0.06323	138
2053.947	21102 - 10002	626	2002	-2096	0.11306	84
2062.099	11101 - 00001	627	2021	-2074	0.03333	114
2063.709	21101 - 10001	636	2032	-2065	0.00276	33
2064.136	13301 - 02201	636	2031	-2072	0.00564	72
2065.864	12201 - 01101	628	2033	-2074	0.01758	171
2075.443	22202 - 11102	626	2037	-2085	0.01176	90
2076.856	11101 - 00001	626	2010	-2145	54.05556	127
2093.345	12201 - 01101	626	2036	-2154	4.92059	214
2094.804	20001 - 01101	628	2061	-2095	0.01038	83
2102.118	20001 - 01101	636	2053	-2140	0.03425	71
2107.084	13301 - 02201	626	2057	-2156	0.33818	172
2110.866	20001 - 01101	627	2086	-2102	0.00099	21
2112.488	21101 - 10001	626	2060	-2161	0.23021	92
2119.022	14401 - 03301	626	2079	-2131	0.01975	98
2120.506	22201 - 11101	626	2082	-2128	0.01548	94
2129.756	20001 - 01101	626	2069	-2189	3.10450	111
2131.805	30002 - 11102	626	2091	-2132	0.00678	43
2136.508	21101 - 02201	636	2109	-2137	0.00156	34
2148.240	30001 - 11101	626	2108	-2149	0.01160	47
2157.675	10012 - 10001	636	2121	-2188	0.00763	42
2165.541	21101 - 02201	626	2110	-2212	0.16577	162
2167.944	21101 - 10002	636	2140	-2157	0.00052	11
2170.850	11112 - 11101	626	2126	-2203	0.04198	100
2180.699	20012 - 20001	626	2161	-2197	0.00055	13
2182.480	20013 - 20002	626	2154	-2208	0.00248	32
2194.115	22201 - 03301	626	2154	-2195	0.00802	69
2205.297	10012 - 10001	628	2176	-2228	0.00488	64
2215.264	21101 - 10002	626	2165	-2237	0.11691	74
2224.657	10012 - 10001	626	2158	-2265	1.22951	69
2225.361	05511 - 05501	636	2204	-2244	0.00134	31
2228.043	13312 - 13302	636	2202	-2251	0.00305	51
2229.724	21113 - 21103	636	2201	-2253	0.00411	58
2230.226	21112 - 21102	636	2214	-2246	0.00071	18
2236.679	04411 - 04401	636	2189	-2270	0.06256	118
2238.570	12211 - 12201	636	2194	-2270	0.03770	103
2239.297	12212 - 12202	636	2192	-2274	0.07091	115
2240.536	20013 - 20003	636	2192	-2274	0.04231	53
2240.753	20011 - 20001	636	2200	-2270	0.01196	45
2242.323	20012 - 20002	636	2196	-2275	0.02562	51
2242.808	02211 - 02201	638	2196	-2275	0.14759	236
2245.273	10011 - 10001	638	2200	-2277	0.05508	104

continued

Table V, continuation 7

2245.496	10012 - 10002	638	2198	-2278	0.08123	109
2248.357	03311 - 03301	636	2184	-2288	1.51871	167
2248.362	01121 - 01111	636	2209	-2278	0.01809	87
2250.606	11111 - 11101	636	2188	-2289	0.95916	152
2250.693	11112 - 11102	636	2185	-2291	1.90892	163
2250.798	02211 - 02201	637	2215	-2279	0.02494	166
2253.046	10012 - 10002	637	2216	-2281	0.01406	83
2253.442	10011 - 10001	637	2219	-2279	0.00917	75
2254.380	01111 - 01101	638	2190	-2293	3.47747	333
2260.051	02211 - 02201	636	2181	-2304	34.58897	205
2260.061	00021 - 00011	636	2202	-2297	0.22775	62
2261.909	10012 - 10002	636	2183	-2306	20.29365	79
2262.453	01111 - 01101	637	2206	-2298	0.62664	272
2262.849	10011 - 10001	636	2186	-2305	12.29448	77
2265.972	00011 - 00001	638	2188	-2308	38.78106	163
2271.760	01111 - 01101	636	2180	-2318	817.84794	237
2273.907	06611 - 06601	626	2241	-2297	0.00536	67
2274.088	00011 - 00001	637	2203	-2315	7.14722	148
2275.804	14411 - 14401	626	2250	-2297	0.00247	46
2277.169	22211 - 22201	626	2258	-2295	0.00114	27
2277.986	30011 - 30001	626	2264	-2294	0.00023	6
2278.322	14412 - 14402	626	2243	-2306	0.00977	79
2280.579	22212 - 22202	626	2250	-2305	0.00524	63
2281.700	22213 - 22203	626	2243	-2310	0.01449	85
2282.690	04411 - 04401	628	2250	-2308	0.01395	146
2283.279	30014 - 30004	626	2245	-2312	0.00846	42
2283.488	00011 - 00001	636	2182	-2331	9598.15028	98
2283.578	30012 - 30002	626	2257	-2306	0.00186	28
2284.279	12211 - 12201	628	2255	-2308	0.00982	126
2285.427	30013 - 30003	626	2253	-2311	0.00376	35
2286.535	05511 - 05501	626	2233	-2322	0.16134	134
2286.800	03321 - 03311	626	2265	-2306	0.00163	35
2287.111	12212 - 12202	628	2257	-2312	0.01124	132
2288.390	13311 - 13301	626	2238	-2322	0.09611	124
2289.569	02211 - 02201	828	2254	-2315	0.01191	84
2289.904	21111 - 21101	626	2242	-2323	0.07101	108
2290.254	11122 - 11112	626	2264	-2312	0.00300	51
2290.501	20013 - 20003	628	2252	-2318	0.01745	87
2290.614	20012 - 20002	628	2256	-2317	0.01017	80
2290.681	13312 - 13302	626	2235	-2327	0.26038	141
2290.972	10011 - 10001	828	2258	-2315	0.00456	39
2293.409	21112 - 21102	626	2240	-2328	0.15630	122
2293.611	21113 - 21103	626	2237	-2331	0.34430	136
2294.879	10012 - 10002	828	2259	-2321	0.00769	44
2295.027	03311 - 03301	628	2242	-2330	0.40463	280
2295.042	01121 - 01111	628	2272	-2315	0.00465	90
2296.848	11111 - 11101	628	2245	-2331	0.32356	250
2299.214	04411 - 04401	626	2230	-2339	4.20855	180
2299.240	02221 - 02211	626	2251	-2332	0.06784	115
2299.415	11112 - 11102	628	2244	-2335	0.68444	276
2301.054	12211 - 12201	626	2234	-2341	2.67856	174
2301.800	01111 - 01101	828	2248	-2335	0.30927	140
2301.909	10021 - 10011	626	2256	-2333	0.02538	50
2302.372	10022 - 10012	626	2253	-2336	0.04233	54
2302.525	20011 - 20001	626	2235	-2342	1.10960	69
2302.964	12212 - 12202	626	2231	-2345	6.36718	185
2305.257	20013 - 20003	626	2234	-2347	3.77753	73

continued

Table V, continuation 8

2306.692	20012 - 20002	626	2237 -2347	2.02918		71
2306.739	11112 - 11102	627	2260 -2339	0.11470		212
2307.383	02211 - 02201	628	2238 -2347	10.49512		374
2307.391	00021 - 00011	628	2259 -2339	0.07873		109
2309.290	10011 - 10001	628	2241 -2348	4.46815		146
2311.668	03311 - 03301	626	2227 -2356	109.93935		218
2311.701	01121 - 01111	626	2246 -2350	1.66896		162
2311.715	10012 - 10002	628	2242 -2351	7.28664		150
2313.773	11111 - 11101	626	2231 -2357	75.17941		211
2314.049	00011 - 00001	828	2245 -2351	3.59815		77
2315.147	02211 - 02201	627	2253 -2353	1.90775		322
2315.235	11112 - 11102	626	2230 -2360	152.95392		219
2317.319	10011 - 10001	627	2256 -2354	0.80461		130
2318.964	10012 - 10002	627	2256 -2357	1.28913		134
2319.738	01111 - 01101	628	2236 -2362	257.87889		446
2322.436	00011 - 00001	728	2261 -2359	1.34887		138
2324.141	02211 - 02201	626	2227 -2371	2838.85708		250
2324.183	00021 - 00011	626	2244 -2366	20.29292		80
2326.598	10011 - 10001	626	2231 -2372	1079.32927		91
2327.433	10012 - 10002	626	2231 -2374	1789.32579		93
2327.581	01111 - 01101	627	2250 -2369	49.68339		400
2332.113	00011 - 00001	628	2236 -2376	3518.85157		192
2336.632	01111 - 01101	626	2227 -2384	73666.25799		278
2340.014	00011 - 00001	627	2249 -2384	647.57535		179
2349.143	00011 - 00001	626	2230 -2397	955357.11615		110
2367.083	10011 - 10002	636	2322 -2395	0.01291		47
2391.161	11111 - 11102	636	2362 -2414	0.00420		58
2415.708	10011 - 10002	628	2393 -2436	0.00229		45
2429.374	10011 - 10002	626	2364 -2467	0.66246		66
2429.468	20012 - 20003	626	2408 -2448	0.00083		18
2458.159	11111 - 11102	626	2418 -2485	0.01525		84
2464.999	21103 - 01101	628	2439 -2493	0.01008		130
2500.760	20003 - 00001	628	2459 -2544	0.13869		115
2524.248	20003 - 00001	627	2499 -2551	0.00428		59
2588.182	20002 - 00001	638	2571 -2607	0.00113		27
2614.248	20002 - 00001	628	2569 -2657	0.23069		119
2618.641	21102 - 01101	628	2590 -2648	0.01488		146
2641.240	20002 - 00001	627	2610 -2673	0.01088		80
2757.178	20001 - 00001	628	2723 -2797	0.03260		98
2775.595	20001 - 00001	627	2762 -2793	0.00062		16
3125.322	30004 - 01101	626	3086 -3172	0.01000		47
3154.604	22203 - 01101	626	3113 -3206	0.03268		101
3181.464	21103 - 00001	626	3133 -3239	0.11155		75
3275.112	30003 - 01101	626	3232 -3317	0.01957		67
3289.698	21102 - 00001	636	3250 -3332	0.00823		44
3339.356	21102 - 00001	626	3280 -3398	1.00026		104
3340.533	22202 - 01101	626	3294 -3394	0.08099		145
3396.895	30002 - 01101	626	3346 -3444	0.04546		70
3398.218	21113 - 11101	626	3373 -3421	0.00284		50
3450.902	13312 - 03301	636	3412 -3481	0.01666		90
3460.466	21113 - 11102	636	3418 -3495	0.04028		99
3465.439	20013 - 10001	626	3412 -3505	0.16788		60
3473.712	12212 - 02201	636	3419 -3513	0.34140		143
3482.235	20013 - 10002	636	3423 -3524	0.44972		65
3482.693	10022 - 00011	636	3456 -3506	0.00188		28
3482.831	21112 - 11101	636	3445 -3511	0.01281		82

continued

Table V, continuation 9

3490.397	10012 - 00001	638	3434 -3528	0.46260	127
3496.165	23313 - 13302	626	3466 -3518	0.00408	58
3497.495	30001 - 01101	636	3453 -3540	0.52628	63
3498.753	11112 - 01101	636	3431 -3544	7.27094	131
3500.672	21101 - 00001	626	3445 -3561	0.68233	100
3504.329	21113 - 11102	628	3476 -3528	0.00943	124
3504.932	14412 - 04401	626	3461 -3538	0.04115	110
3506.713	31114 - 21103	626	3473 -3534	0.00842	73
3508.376	10012 - 00001	637	3461 -3543	0.07672	107
3509.216	21112 - 11101	628	3492 -3526	0.00193	48
3511.419	12212 - 02201	628	3465 -3547	0.17960	244
3517.322	20012 - 10001	636	3460 -3554	0.17683	61
3518.662	22213 - 12202	626	3469 -3555	0.12137	125
3524.203	31113 - 21102	626	3498 -3546	0.00300	51
3525.204	10012 - 00001	828	3477 -3556	0.05860	58
3527.615	30014 - 20003	626	3476 -3565	0.09161	57
3527.737	10012 - 00001	636	3446 -3577	94.17139	85
3527.767	22212 - 12201	626	3484 -3559	0.03200	100
3528.057	13312 - 03301	626	3465 -3568	1.10940	163
3531.835	20013 - 10002	628	3481 -3567	0.18061	117
3533.947	11122 - 01111	626	3496 -3564	0.01652	86
3538.778	11112 - 01101	628	3473 -3578	4.44759	341
3539.017	20012 - 10001	628	3489 -3569	0.07566	108
3542.604	21113 - 11102	626	3476 -3584	1.47184	85
3543.095	40002 - 11102	626	3502 -3583	0.09824	58
3549.213	20013 - 10002	627	3510 -3579	0.02195	91
3550.717	30012 - 20001	626	3506 -3579	0.01686	47
3552.854	12212 - 02201	626	3476 -3598	29.39272	203
3555.909	21112 - 11101	626	3492 -3593	0.99325	154
3556.775	30013 - 20002	626	3506 -3591	0.05511	55
3558.705	11112 - 01101	627	3502 -3595	0.66658	272
3563.324	20012 - 10001	627	3525 -3589	0.01300	83
3566.070	10022 - 00011	626	3509 -3604	0.20784	62
3568.215	20013 - 10002	626	3490 -3615	31.80315	81
3571.141	10012 - 00001	628	3491 -3612	52.18823	165
3580.326	11112 - 01101	626	3490 -3628	779.87245	235
3587.550	10011 - 00001	638	3527 -3624	0.70266	131
3589.064	10021 - 00011	636	3555 -3614	0.00380	36
3589.650	20012 - 10001	626	3506 -3628	16.59292	79
3591.251	10012 - 00001	627	3519 -3631	8.40531	149
3608.559	10011 - 00001	637	3557 -3642	0.12564	112
3612.842	10012 - 00001	626	3509 -3661	10397.26485	99
3621.287	20011 - 10001	636	3562 -3659	0.28276	63
3621.557	20012 - 10002	636	3555 -3655	0.43485	65
3623.386	21112 - 11102	636	3576 -3653	0.04267	100
3625.165	21111 - 11101	636	3581 -3656	0.03177	95
3632.911	10011 - 00001	636	3543 -3675	159.96019	86
3638.065	10011 - 00001	828	3594 -3670	0.03895	55
3639.220	11111 - 01101	636	3561 -3680	14.99625	191
3641.570	12211 - 02201	636	3580 -3678	0.57754	151
3641.676	13311 - 03301	636	3599 -3671	0.02329	97
3645.436	20012 - 10002	628	3592 -3678	0.18657	117
3656.819	21112 - 11102	628	3625 -3681	0.01340	138
3659.273	02211 - 00001	626	3584 -3714	1.00696	79
3667.064	20012 - 10002	627	3622 -3696	0.03289	97
3667.548	10021 - 00011	626	3606 -3704	0.36867	64
3675.134	10011 - 00001	628	3599 -3719	47.78956	164

continued

Table V, continuation 10

3675.694	11121 - 01111	626	3632 -3706	0.03018	95
3676.709	30012 - 20002	626	3623 -3712	0.07782	57
3676.740	20011 - 10001	628	3627 -3712	0.16362	116
3677.708	21111 - 11101	628	3647 -3702	0.01194	135
3679.552	30013 - 20003	626	3622 -3710	0.08420	57
3682.095	31113 - 21103	626	3648 -3706	0.00686	70
3683.814	11111 - 01101	628	3619 -3723	3.87816	336
3684.321	31112 - 21102	626	3654 -3709	0.00527	64
3687.475	12211 - 02201	628	3640 -3720	0.14164	236
3692.426	20012 - 10002	626	3606 -3731	38.37714	81
3692.903	20011 - 10001	627	3651 -3724	0.02749	95
3693.346	10011 - 00001	627	3620 -3734	10.19757	151
3700.295	21112 - 11102	626	3629 -3738	3.09851	170
3702.083	11111 - 01101	627	3644 -3739	0.76960	278
3703.152	31111 - 21101	626	3679 -3724	0.00246	46
3703.470	22212 - 12202	626	3650 -3737	0.12639	127
3704.244	23312 - 13302	626	3674 -3727	0.00430	59
3705.946	30011 - 20001	626	3658 -3740	0.04601	53
3711.476	20011 - 10001	626	3633 -3758	31.18729	81
3712.534	23311 - 13301	626	3688 -3734	0.00240	44
3713.720	21111 - 11101	626	3648 -3755	2.41894	167
3713.805	22211 - 12201	626	3664 -3748	0.09128	120
3714.783	10011 - 00001	626	3610 -3763	15796.07761	99
3723.249	11111 - 01101	626	3629 -3770	1270.12882	241
3723.800	15511 - 05501	626	3699 -3744	0.00200	41
3725.522	20011 - 10002	636	3685 -3752	0.00756	42
3726.355	14411 - 04401	626	3677 -3760	0.07858	122
3726.647	12211 - 02201	626	3646 -3770	50.58909	209
3727.359	13311 - 03301	626	3661 -3767	2.00935	170
3783.158	20011 - 10002	628	3760 -3804	0.00255	47
3799.487	30012 - 20003	626	3772 -3821	0.00187	28
3814.251	20011 - 10002	626	3751 -3855	0.66153	67
3856.658	30003 - 00001	628	3823 -3889	0.01548	86
3858.105	21111 - 11102	626	3818 -3888	0.02067	88
3987.609	30002 - 00001	628	3956 -4021	0.01438	85
4005.946	00021 - 01101	626	3934 -4029	0.05019	78
4416.150	31104 - 00001	626	4389 -4454	0.00197	24
4529.869	40004 - 01101	626	4543 -4558	0.00049	10
4578.089	32203 - 01101	626	4591 -4608	0.00104	21
4591.118	31103 - 00001	626	4548 -4635	0.01493	61
4614.780	01121 - 01101	628	4583 -4634	0.00884	122
4639.504	00021 - 00001	628	4580 -4663	0.12357	113
4655.203	00021 - 00001	627	4614 -4677	0.01215	81
4685.775	30014 - 10002	636	4662 -4709	0.00144	25
4687.797	30014 - 10001	626	4654 -4718	0.00583	40
4692.180	20013 - 00001	638	4673 -4711	0.00140	32
4708.526	21113 - 01101	636	4669 -4743	0.02919	94
4722.629	32214 - 12202	626	4733 -4737	0.00019	5
4733.542	23313 - 03301	626	4694 -4760	0.01207	84
4735.614	40015 - 20003	626	4714 -4757	0.00113	22
4743.693	21113 - 01101	628	4706 -4773	0.03233	176
4748.063	20013 - 00001	636	4691 -4792	0.46881	65
4753.450	31102 - 00001	626	4714 -4795	0.01099	58
4755.707	31114 - 11102	626	4712 -4791	0.04140	100
4768.553	22213 - 02201	626	4714 -4807	0.31338	141
4784.676	20023 - 00011	626	4764 -4805	0.00100	20
4786.703	31113 - 11101	626	4751 -4813	0.00991	75

continued

Table V, continuation 11

4790.573	30014 - 10002	626	4735 -4833	0.38174	63
4791.261	20013 - 00001	628	4739 -4826	0.21364	119
4807.695	21113 - 01101	626	4736 -4854	6.64294	183
4808.185	40002 - 01101	626	4764 -4851	0.22048	65
4814.570	20012 - 00001	638	4777 -4840	0.01285	83
4821.500	20013 - 00001	627	4774 -4856	0.07405	107
4839.734	30013 - 10001	626	4782 -4873	0.15378	59
4853.623	20013 - 00001	626	4774 -4902	77.80096	83
4871.446	21112 - 01101	636	4815 -4907	0.23733	130
4887.385	20012 - 00001	636	4813 -4926	2.97523	73
4887.986	12212 - 00001	626	4827 -4937	0.04586	61
4896.182	21112 - 01101	628	4851 -4927	0.08795	204
4904.861	20012 - 00001	628	4841 -4940	1.11940	135
4910.599	20022 - 00011	626	4872 -4938	0.00756	42
4912.163	40014 - 20003	626	4879 -4936	0.00348	35
4920.197	32213 - 12202	626	4893 -4942	0.00322	52
4922.547	40013 - 20002	626	4889 -4946	0.00339	35
4925.013	20011 - 00001	638	4898 -4947	0.00367	57
4928.916	21112 - 01101	627	4896 -4954	0.01347	138
4931.089	31113 - 11102	626	4879 -4964	0.10332	115
4937.312	40012 - 20001	626	4920 -4954	0.00049	12
4939.350	20012 - 00001	627	4883 -4972	0.23058	118
4941.621	23312 - 03301	626	4898 -4972	0.03282	104
4942.510	30013 - 10002	626	4872 -4978	1.31966	69
4946.821	31112 - 11101	626	4899 -4979	0.05226	103
4953.361	22212 - 02201	626	4890 -4991	0.89722	158
4959.668	30012 - 10001	626	4892 -4996	0.82769	67
4965.385	21112 - 01101	626	4884 -5007	24.49150	198
4977.835	20012 - 00001	626	4881 -5018	351.92470	89
4991.350	20011 - 00001	636	4920 -5030	2.11943	71
5013.780	21111 - 01101	636	4959 -5048	0.17029	123
5028.536	20021 - 00011	626	5000 -5052	0.00238	31
5028.787	22211 - 02201	636	5006 -5048	0.00195	40
5042.584	20011 - 00001	628	4992 -5080	0.22656	119
5061.779	12211 - 00001	626	4999 -5109	0.05211	61
5062.444	30012 - 10002	626	5002 -5097	0.25375	62
5064.674	21111 - 01101	628	5029 -5093	0.02463	162
5068.930	20011 - 00001	627	5023 -5103	0.06284	105
5091.207	31112 - 11102	626	5048 -5120	0.02311	91
5099.660	20011 - 00001	626	5017 -5148	108.99684	85
5114.898	30011 - 10001	626	5058 -5156	0.30176	63
5123.195	21111 - 01101	626	5050 -5168	10.29872	187
5126.968	31111 - 11101	626	5086 -5159	0.02680	93
5139.399	22211 - 02201	626	5080 -5177	0.43642	148
5151.504	23311 - 03301	626	5112 -5180	0.01718	91
5168.600	01121 - 00001	636	5142 -5188	0.00314	42
5217.673	30011 - 10002	626	5175 -5251	0.02179	49
5247.834	10022 - 01101	626	5208 -5269	0.00975	61
5291.133	02221 - 01101	626	5250 -5315	0.02682	125
5315.714	01121 - 00001	626	5248 -5342	0.39742	92
5349.312	10021 - 01101	626	5316 -5368	0.00460	50
5584.394	00031 - 10001	626	5560 -5599	0.00083	18
5687.170	00031 - 10002	626	5652 -5703	0.00197	29
5858.024	10022 - 00001	628	5830 -5876	0.00282	50
5951.604	30014 - 00001	636	5922 -5980	0.00329	35
5959.956	10021 - 00001	628	5935 -5977	0.00240	46

continued

Table V, continuation 12

5972.520	32214 - 02201	626	5953	-5991	0.00131	30
5998.572	40015 - 10002	626	5970	-6025	0.00285	32
6020.797	31114 - 01101	626	5977	-6058	0.05285	103
6072.345	40014 - 10001	626	6059	-6088	0.00023	6
6075.981	30014 - 00001	626	6019	-6120	0.52309	65
6088.220	31113 - 01101	636	6069	-6106	0.00113	27
6119.623	30013 - 00001	636	6073	-6152	0.02880	51
6127.781	30013 - 00001	628	6086	-6154	0.02334	93
6148.416	41114 - 11102	626	6158	-6163	0.00023	6
6170.088	32213 - 02201	626	6133	-6198	0.01191	82
6175.121	40014 - 10002	626	6130	-6206	0.02218	49
6175.954	30013 - 00001	627	6152	-6195	0.00224	44
6196.179	31113 - 01101	626	6137	-6233	0.33332	135
6205.505	40013 - 10001	626	6160	-6232	0.01420	47
6227.919	30013 - 00001	626	6153	-6265	4.60947	73
6241.972	30012 - 00001	636	6190	-6271	0.04589	53
6243.580	31112 - 01101	636	6217	-6265	0.00323	52
6254.594	30012 - 00001	628	6218	-6282	0.01357	84
6298.114	30012 - 00001	627	6277	-6317	0.00165	36
6308.281	40013 - 10002	626	6260	-6335	0.02050	49
6346.263	40012 - 10001	626	6303	-6376	0.01282	47
6347.853	30012 - 00001	626	6273	-6386	4.57936	73
6356.297	31112 - 01101	626	6297	-6393	0.34437	137
6359.285	32212 - 02201	626	6321	-6387	0.01239	82
6363.616	30011 - 00001	636	6323	-6394	0.01249	46
6388.085	41101 - 00001	626	6355	-6424	0.00213	30
6466.439	20023 - 01101	626	6464	-6466	0.00012	3
6503.082	30011 - 00001	626	6445	-6546	0.59279	65
6532.655	40011 - 10001	626	6507	-6556	0.00169	27
6536.444	31111 - 01101	626	6489	-6571	0.06199	106
6537.959	11122 - 00001	626	6493	-6562	0.02197	69
6562.442	32211 - 02201	626	6547	-6577	0.00059	15
6679.707	11121 - 00001	626	6631	-6704	0.02800	72
6745.114	01131 - 01101	636	6698	-6763	0.01282	82
6780.212	00031 - 00001	636	6705	-6797	0.16370	60
6870.799	11132 - 11102	626	6852	-6884	0.00071	18
6885.166	01131 - 01101	628	6894	-6896	0.00037	10
6897.754	02231 - 02201	626	6838	-6915	0.04153	106
6905.769	10031 - 10001	626	6850	-6922	0.01479	47
6907.144	10032 - 10002	626	6846	-6924	0.02522	51
6922.210	00031 - 00001	628	6862	-6938	0.05165	103
6935.135	01131 - 01101	626	6846	-6952	1.10889	155
6945.608	00031 - 00001	627	6901	-6962	0.01064	79
6972.579	00031 - 00001	626	6860	-6989	14.59010	78
7283.981	40015 - 00001	626	7258	-7309	0.00197	29
7413.506	41114 - 01101	626	7389	-7435	0.00247	46
7460.530	40014 - 00001	626	7411	-7494	0.03781	53
7481.570	40013 - 00001	636	7464	-7497	0.00048	12
7583.251	41113 - 01101	626	7550	-7608	0.00688	70
7593.690	40013 - 00001	626	7536	-7624	0.10180	57
7734.448	40012 - 00001	626	7687	-7766	0.02791	51
7757.620	41112 - 01101	626	7740	-7773	0.00075	19
7901.479	21122 - 00001	626	7898	-7917	0.00069	15
7920.840	40011 - 00001	626	7896	-7944	0.00166	27
7981.180	10032 - 00001	636	7948	-7998	0.00196	29
8089.028	10031 - 00001	636	8043	-8105	0.00680	41

continued

Table V, continuation 13

8103.581	20033 - 10002	626	8087 -8117	0.00032	8
8120.106	10032 - 00001	628	8129 -8131	0.00019	5
8135.889	11132 - 01101	626	8082 -8154	0.02698	93
8192.552	10032 - 00001	626	8107 -8210	0.43071	65
8220.363	10031 - 00001	628	8229 -8232	0.00019	5
8231.561	20032 - 10002	626	8202 -8246	0.00123	23
8243.165	20031 - 10001	626	8219 -8257	0.00078	17
8254.798	12231 - 02201	626	8237 -8267	0.00050	13
8276.766	11131 - 01101	626	8214 -8293	0.05392	103
8293.953	10031 - 00001	626	8206 -8310	0.61321	65
9388.990	20033 - 00001	626	9350 -9408	0.00385	36
9516.970	20032 - 00001	626	9457 -9533	0.02307	49
9631.350	20031 - 00001	626	9583 -9649	0.00904	43

O_3 Molecule: number of lines = 50080

Band Centers	Isotope	Vibrational Band upper	lower	Frequency min	max	number lines	Sum of Intensity	
	666	000-	000	0-	191	3982	4.387E-19	N
698.3443	666	020-	010	573-	865	4591	4.164E-20	
700.9314	666	010-	000	560-	895	6340	6.283E-19	
1007.650	666	101-	100	948-	1036	1185	6.152E-20	
1007.996	686	001-	000	956-	1037	993	2.495E-20	
1015.808	666	002-	001	958-	1048	1534	1.743E-19	
1025.596	666	011-	010	969-	1068	1544	4.503E-19	
1028.096	668	001-	000	971-	1059	1149	5.073E-20	
1042.0843	666	001-	000	919-	1244	6992	1.354E-17	N
1095.329	666	110-	010	979-	1174	901	1.104E-20	
1103.1403	666	100-	000	942-	1271	6671	5.255E-19	N
1726.5277	666	011-	000	1657-	1910	1709	5.373E-20	
1796.2606	666	110-	000	1681-	1927	2137	2.266E-20	
2057.892	666	002-	000	1945-	2140	2164	1.107E-19	
2084.3132	666	111-	010	2029-	2107	1469	3.743E-20	N
2110.785	666	101-	000	1968-	2164	2165	1.134E-18	
2201.157	666	200-	000	2058-	2270	1530	3.000E-20	
2785.2446	666	111-	000	2735-	2807	1449	3.140E-20	N
3041.200	666	003-	000	2962-	3056	1575	1.105E-19	

continued

fundamental at 667 cm^{-1} and the two hot bands at 618 and 721 cm^{-1}, have been appended. These come from the room temperature studies of Hoke *et al.*[19] The corresponding modification to the line shape form factor, $f(\nu,\nu_{if})$, yields

$$f(\nu,\nu_{if}) = \frac{1}{\pi}\frac{\gamma_{if} + y_{if}(\nu - \nu_{if})}{(\nu - \nu_{if})^2 + \gamma_{if}^2}, \quad (5)$$

where y_{if} is the coupling coefficient, ν_{if} is the frequency of the transition, and γ_{if} is the air-broadened half-width. Equation (5) is the result of a perturbation calculation to first order.[20] The y_{if} coefficients have been introduced at this time in the field of the pressure shift on the compilation. Note that when the coupling coefficient is zero, $f(\nu,\nu_{if})$ reduces to the Lorentz form factor.

The y_{if} values on the current edition apply only to a temperature of 296 K; atmospheric calculations through layers with different temperatures are certain to yield invalid results. A scheme for temperature

Table V, continuation 14

N_2O Molecule: number of lines = 24125

Band Centers	Isotope	Vibrational Band upper	lower	Frequency min	max	number lines	Sum of Intensity	
	446	0000-	0000	0-	46	54	8.292E-21	N
	456	0000-	0000	5-	46	49	3.077E-23	N
	546	0000-	0000	4-	46	51	2.985E-23	N
	446	0110-	0110	2-	46	104	9.509E-22	N
	446	0200-	0200	5-	46	49	2.835E-23	N
	446	0220-	0220	5-	46	97	5.454E-23	N
	446	1000-	1000	6-	45	47	1.590E-23	N
571.320	446	0310-	0220	527-	617	294	2.484E-21	
575.5	456	0110-	0000	541-	612	128	3.504E-21	
579.364	446	0200-	0110	527-	637	195	5.561E-20	
580.934	446	0310-	0200	538-	623	150	6.567E-21	
584.1	448	0110-	0000	555-	616	116	1.890E-21	
585.320	546	0110-	0000	552-	622	129	3.499E-21	
586.3	447	0110-	0000	586-	602	32	1.820E-22	
588.768	446	0110-	0000	523-	658	240	9.857E-19	
588.978	446	0220-	0110	535-	650	384	1.112E-19	
589.168	446	0330-	0220	546-	635	297	9.328E-21	
595.361	446	1110-	1000	564-	630	118	2.103E-21	
696.140	446	1000-	0110	659-	728	123	2.856E-21	
938.8534	446	0001-	1000	881-	984	123	9.780E-22	N
1055.6245	446	0001-	0200	999-	1089	107	2.893E-22	N
1144.3334	456	0200-	0000	1099-	1195	113	4.780E-22	N
1153.3768	446	0420-	0220	1104-	1208	294	3.545E-21	N
1154.4408	446	0400-	0200	1104-	1208	123	2.483E-21	N
1155.1399	448	0200-	0000	1109-	1207	123	1.335E-21	N
1159.9717	546	0200-	0000	1114-	1212	120	1.200E-21	N
1160.2973	446	0310-	0110	1103-	1226	356	5.182E-20	N
1168.1323	446	0200-	0000	1105-	1239	159	2.877E-19	N
1177.0931	446	1200-	1000	1131-	1229	116	9.659E-22	N
1177.7446	446	0220-	0000	1123-	1248	136	1.251E-21	N
1246.8846	448	1000-	0000	1184-	1297	142	1.673E-20	N
1255.7114	448	1110-	0110	1205-	1299	264	1.968E-21	N
1264.7047	447	1000-	0000	1207-	1310	127	3.300E-21	N
1269.8920	546	1000-	0000	1203-	1321	145	2.859E-20	N
1277.4549	546	1110-	0110	1223-	1323	282	3.297E-21	N
1278.4361	446	2000-	1000	1211-	1330	143	3.115E-20	N
1280.3541	456	1000-	0000	1211-	1331	143	3.221E-20	N
1284.7573	456	1110-	0110	1228-	1330	282	3.940E-21	N
1284.9033	446	1000-	0000	1208-	1341	159	8.248E-18	N
1285.5879	446	2110-	1110	1231-	1331	279	3.805E-21	N
1291.4979	446	1110-	0110	1215-	1349	418	9.440E-19	N
1293.8642	446	1200-	0200	1226-	1345	141	2.793E-20	N
1297.0540	446	1220-	0220	1231-	1349	360	5.363E-20	N
1297.1477	446	1310-	0310	1241-	1342	277	3.887E-21	N
1301.8084	446	1330-	0330	1248-	1347	292	3.564E-21	N
1395.2071	446	2000-	0200	1345-	1427	97	1.375E-22	N
1620.5479	446	0111-	0220	1580-	1652	260	2.625E-22	N
1630.1603	446	0111-	0200	1585-	1662	143	1.457E-22	N
1634.9889	446	0001-	0110	1581-	1673	172	2.778E-21	N

continued

Table V, continuation 15

1733.8051	446	0400-	0110	1694-	1775	147	1.727E-22 N
1742.3536	446	0420-	0110	1706-	1779	252	2.508E-22 N
1749.0651	446	0310-	0000	1701-	1796	172	2.177E-21 N
1839.9361	448	1110-	0000	1807-	1863	105	4.080E-23 N
1860.1913	456	1110-	0000	1819-	1889	125	7.959E-23 N
1862.7670	546	1110-	0000	1824-	1888	117	7.300E-23 N
1868.4682	446	1310-	0220	1826-	1894	226	1.387E-22 N
1873.2286	446	1200-	0110	1819-	1910	161	7.733E-22 N
1878.0806	446	1310-	0200	1838-	1903	116	6.981E-23 N
1880.2657	446	1110-	0000	1813-	1925	200	2.118E-20 N
1880.9503	446	2110-	1000	1844-	1904	107	4.642E-23 N
1886.0307	446	1220-	0110	1832-	1923	312	2.282E-21 N
1890.9760	446	1330-	0220	1853-	1918	224	1.296E-22 N
1974.5715	446	2000-	0110	1918-	2006	156	4.204E-22 N
2079.0746	446	0201-	1000	2048-	2108	66	1.923E-23 N
2164.1644	456	0111-	0110	2093-	2206	332	2.220E-20 N
2177.6568	456	0001-	0000	2094-	2223	155	1.824E-19 N
2181.3724	446	0331-	0330	2111-	2223	338	1.815E-20 N
2181.7137	446	1111-	1110	2113-	2222	318	1.211E-20 N
2182.1823	446	0311-	0310	2111-	2224	332	2.048E-20 N
2187.3906	546	0111-	0110	2117-	2228	338	2.220E-20 N
2193.6210	446	0002-	0001	2134-	2231	117	1.138E-21 N
2195.3966	446	0221-	0220	2112-	2240	404	3.233E-19 N
2195.8457	446	0201-	0200	2111-	2241	155	1.708E-19 N
2195.9158	446	1001-	1000	2114-	2239	151	1.053E-19 N
2201.6053	546	0001-	0000	2118-	2245	157	1.824E-19 N
2202.7922	448	0111-	0110	2135-	2242	326	1.287E-20 N
2206.0063	447	0111-	0110	2146-	2243	269	2.329E-21 N
2209.5247	446	0111-	0110	2122-	2255	432	5.701E-18 N
2216.7112	448	0001-	0000	2137-	2259	155	1.049E-19 N
2220.0735	447	0001-	0000	2147-	2261	142	2.098E-20 N
2223.7568	446	0001-	0000	2121-	2271	180	5.005E-17 N
2181.6967	446	0600-	1000	2148-	2228	8	9.409E-23 N
2189.5466	446	0620-	1000	2168-	2217	2	3.529E-23 N
2309.0455	446	0510-	0110	2259-	2369	292	5.392E-21 N
2322.5731	446	0400-	0000	2269-	2387	140	2.113E-20 N
2331.1215	446	0420-	0000	2284-	2399	116	2.404E-22 N
2411.5068	448	1200-	0000	2360-	2456	121	1.489E-21 N
2431.3226	456	1200-	0000	2380-	2475	112	7.204E-22 N
2435.7273	447	1200-	0000	2392-	2475	101	1.640E-22 N
2439.6247	546	1200-	0000	2387-	2486	122	1.202E-21 N
2452.8106	446	1400-	0200	2397-	2499	122	2.073E-21 N
2453.8452	446	1420-	0220	2400-	2501	286	2.960E-21 N
2457.4449	446	1310-	0110	2391-	2513	352	4.404E-20 N
2461.9965	446	1200-	0000	2388-	2521	159	2.747E-19 N
2463.3484	446	2200-	1000	2409-	2511	122	2.042E-21 N
2474.7987	446	1220-	0000	2415-	2536	130	1.065E-21 N
2491.1871	448	2000-	0000	2431-	2532	127	2.911E-21 N
2524.6727	447	2000-	0000	2471-	2561	111	5.235E-22 N
2534.5321	546	2000-	0000	2470-	2575	129	3.975E-21 N
2551.4678	446	3000-	1000	2483-	2594	132	6.596E-21 N
2552.4083	456	2000-	0000	2486-	2591	126	4.121E-21 N
2563.3394	446	2000-	0000	2477-	2609	159	1.194E-18 N

continued

Table V, continuation 16

2509.1303	448	2110-	0110	2464-	2544	200	2.407E-22 N
2550.2700	546	2110-	0110	2501-	2586	210	3.384E-22 N
2561.5444	456	2110-	0110	2509-	2596	212	4.027E-22 N
2577.0857	446	2110-	0110	2498-	2623	376	1.238E-19 N
2580.1195	446	2200-	0200	2513-	2619	126	3.246E-21 N
2586.7349	446	2310-	0310	2537-	2621	202	3.072E-22 N
2588.3078	446	2220-	0220	2524-	2629	308	6.386E-21 N
2763.1154	446	0311-	0200	2762-	2763	14	6.341E-23
2770.5399	446	0331-	0220	2768-	2789	86	4.756E-22
2775.2101	446	0201-	0110	2735-	2806	130	3.931E-21
2784.3733	446	0221-	0110	2743-	2818	257	8.963E-21
2798.2926	446	0111-	0000	2739-	2837	177	8.065E-20
3342.491	446	0311-	0110	3293-	3380	210	1.555E-20
3363.974	446	0201-	0000	3303-	3406	124	8.829E-20
3430.95	456	1001-	0000	3377-	3460	99	6.236E-21
3439.1	448	1001-	0000	3391-	3466	95	3.442E-21
3443.659	546	1001-	0000	3391-	3472	101	6.241E-21
3445.921	446	2001-	1000	3393-	3475	99	6.515E-21
3462.030	446	1201-	0200	3410-	3491	97	5.582E-21
3464.713	446	1221-	0220	3413-	3494	210	1.040E-20
3466.54	446	3110-	1110	2514-	2604	222	5.673E-22
3473.212	446	1111-	0110	3402-	3506	296	1.919E-19
3480.821	446	1001-	0000	3392-	3514	147	1.732E-18
3620.941	446	1400-	0000	3580-	3661	96	4.886E-21
3747.031	446	2310-	0110	3703-	3780	178	4.991E-21
3748.252	446	2200-	0000	3691-	3788	116	3.521E-20
3836.373	446	3000-	0000	3768-	3870	123	7.286E-20
3857.612	446	3110-	0110	3810-	3888	186	6.838E-21
4061.979	446	1111-	0000	4032-	4084	90	8.157E-22
4388.928	446	0112-	0110	4337-	4413	184	6.711E-21
4417.379	446	0002-	0000	4342-	4443	121	6.074E-20
4335.798	446	2310-	0000	4308-	4359	86	7.212E-22
4630.164	446	1201-	0000	4578-	4661	99	5.943E-21
4730.408	446	2111-	0110	4683-	4755	168	3.959E-21
4730.828	446	2001-	0000	4659-	4756	117	3.900E-20
4977.695	446	0112-	0000	4951-	4997	76	5.716E-22
5026.34	446	3200-	0000	4980-	5055	89	2.511E-21
5105.65	446	4000-	0000	5057-	5132	89	2.511E-21

continued

scaling of the coupling coefficients will be included in a future edition of HITRAN.

C. O_3

The line parameters compilation for the ozone molecule has been expanded and improved considerably since the last edition. This includes updates of several bands as well as several new bands. The following discussion summarizes the new results in the current edition and also reports on several more recent studies which further improve the O_3 line parameters.

The ν_1 and ν_3 $^{16}O_3$ line parameters have been updated according to the recent analysis by Pickett *et al.*[21] of high resolution laboratory microwave and 10-μm infrared measurements (0.005-cm^{-1} resolution). The analysis includes an expanded consideration of the Coriolis coupling coefficients for line positions and intensities. While the previous ν_3 total band intensity has been retained, the ν_1 total band intensity has been revised from 6.711×10^{-19} to 5.255×10^{-19} cm^{-1}/(molec · cm^{-2}). The new line positions are accurate to 0.0006 cm^{-1} and the intensities to 10%. This study[21] also provided the new pure rotation O_3 lines on the current edition which are based on a considerably improved dipole moment expansion.

It should be noted that in the 10-μm region, only the ν_1 and ν_3 lines of the principal isotope $^{16}O_3$ have been revised, while the isotopic and hot band lines have

Table V, continuation 17

Band Centers	Isotope	Vibrational Band upper	lower	Frequency min	max	number lines	Sum of Intensity
	CO Molecule: number of lines = 574						
	26	0-	0	3-	134	35	1.828E-20
	36	0-	0	14-	96	23	1.922E-22
	28	0-	0	25-	74	14	2.975E-23
2092.1231	28	1-	0	1968-	2189	61	1.909E-20
2096.0674	36	1-	0	1958-	2201	67	1.052E-19
2116.2957	27	1-	0	2008-	2205	53	3.541E-21
2116.7912	26	2-	1	2025-	2195	45	5.698E-22
2143.2716	26	1-	0	1968-	2267	79	9.813E-18
4159.0272	28	2-	0	4088-	4217	36	1.357E-22
4166.8198	36	2-	0	4065-	4236	47	7.813E-22
4206.7792	27	2-	0	4224-	4244	7	8.034E-24
4260.0627	26	2-	0	4109-	4347	64	7.522E-20
6350.4396	26	3-	0	6253-	6410	43	4.827E-22

continued

been retained from previous editions. These isotopic lines are based on crude approximations and, while satisfactory for low resolution spectra, cannot reproduce high resolution spectra. Fortunately, more recent studies by Flaud *et al.*[22] and Camy-Peyret *et al.*[23] provide line positions and intensities for the ν_1 and ν_3 bands of $^{16}O^{18}O^{16}O$ and $^{16}O^{16}O^{18}O$, as well as a revised set for the principal isotope.[24] These studies are based on new high resolution (0.005-cm^{-1}) laboratory spectra of natural and oxygen-18 enriched ozone, and include high-order calculations for positions and intensities. These studies allowed the identification of individual isotopic O_3 lines in the atmospheric spectrum as reported by Rinsland *et al.*[25] Unfortunately, these parameters were not available in time for the present edition of the HITRAN database; they will be included in the next update and can be obtained from the authors if necessary before that release.

In the 2800-cm^{-1} region, new line parameters for the important $\nu_1 + \nu_2 + \nu_3$ combination band have been updated on the compilation. These are a slightly revised set of an earlier work, as described by Barbe *et al.*,[26] with line positions accurate to 0.004 cm^{-1}. The line intensities are based on a set of measured line intensities near 2776 cm^{-1} by Meunier *et al.*,[27] with rigid rotor intensity calculations. The estimated accuracy is between 5% and 25%.

In the 3000-cm^{-1} region, it should be noted that the line parameters originate from very early approximate calculations and do not agree with high resolution spectra. Further work on the analysis of the interacting states $2\nu_1 + \nu_3$, $\nu_1 + 2\nu_3$, $3\nu_3$, and $3\nu_1$ is needed.

The hot band $\nu_1 + \nu_2 + \nu_3 - \nu_2$, which also contributes to the atmospheric spectrum in the 5-μm region in addition to the $2\nu_3$, $\nu_1 + \nu_3$, and $2\nu_1$ bands, has been added to the compilation, as described by Goldman and Barbe.[28] The hot band line parameters have been derived from 0.03-cm^{-1} resolution laboratory spectra and provide line positions accurate to 0.004 cm^{-1}. The line intensities were derived as rigid rotor intensities, normalized to the $\nu_1 + \nu_3$ total band intensity multiplied by a ν_2 population factor. Some limitations, depending on the quantum numbers, should be noted.[26,28] It is estimated that the individual line intensities are accurate to 10–30%.

The line parameters for the ν_2 and $2\nu_2 - \nu_2$ bands have not been updated for this edition. However, these will soon be superseded by the newly derived line parameters by Pickett *et al.*[29] This study, based on high resolution laboratory spectra in the microwave and infrared, involves a detailed theoretical analysis which provides line positions accurate to 0.0006 cm^{-1} and absolute intensities accurate to 5% in the range of the fitted data.

The $2\nu_2$ O_3 lines in the 1400-cm^{-1} region are observable in atmospheric spectra, as reported by Goldman *et al.*,[30,31] but parameters are not included in the current compilation. Based on the available spectroscopic constants of the (000) and (020) levels, line parameters have been generated and compared with atmospheric spectra.[31] It is found that while the calculated line positions are accurate to 0.004 cm^{-1}, there are considerable disagreements in the individual intensities. Thus a more refined intensity analysis is needed. In addition, new analyses of the $\nu_1 + \nu_2$ and $\nu_2 + \nu_3$ bands of $^{16}O_3$ have been completed,[32] and updated line parameters are expected to be available soon.

Air-broadened halfwidths were revised for all ozone transitions present on the database. The values up to $J'' = 35$ were from the calculations of Gamache and Rothman[33] scaled to air by the recommended factor, 0.95.[34] Average values were obtained for $J'' > 35$ by

Table V, continuation 18

CH$_4$ Molecule: number of lines = 17774

Band Centers	Isotope	Vibrational Band upper	lower	Frequency min	max	number lines	Sum of Intensity	
	212	Ground-	Ground	7-	101	80	4.241E-26	
1161.0880	212	V6-	Ground	1042-	1254	487	1.525E-21	N
1302.7719	311	00000111-	00000000	1183-	1384	353	5.544E-20	N
1306.836	212	V3-	Ground	1173-	1418	318	1.268E-21	N
1310.7606	211	00000111-	00000000	1071-	1544	1420	5.041E-18	
1472.	212	V5-	Ground	1343-	1600	216	2.647E-22	N
1533.3367	211	01100001-	00000000	1378-	1735	810	5.503E-20	
1533.526	311	01100001-	00000000	1417-	1645	69	3.153E-22	N
1720.	211	00011001-	00000111	1530-	1932	462	1.537E-21	N
	212	2V6-	Ground	2088-	2434	612	1.148E-22	N
2596.	311	00000222-	00000000	2461-	2728	36	1.771E-22	N
2596.	211	00000202-	00000000	2458-	2682	41	5.420E-22	
2612.	211	00000222-	00000000	2255-	2848	1266	5.500E-20	N
2822.	311	01100112-	00000000	2659-	2999	208	2.805E-21	N
2830.	211	01100112-	00000000	2573-	3168	2300	3.768E-19	N
2917.	211	10000000-	00000000	2764-	3068	52	1.159E-21	
3000.	212	2V5-	Ground	2902-	3130	41	4.894E-22	N
3000.	212	V4-	Ground	2902-	3147	272	8.867E-21	N
3000.	212	V1-	Ground	2902-	3071	31	5.391E-22	N
3000.	311	00011112-	00000111	3034-	3091	12	5.906E-23	N
3009.049	311	00011001-	00000000	2832-	3168	355	8.549E-20	N
3010.	211	01111002-	01100001	2898-	3106	264	6.801E-21	N
3010.	211	00011112-	00000111	2880-	3136	712	4.445E-20	N
3018.9205	211	00011001-	00000000	2809-	3210	1903	1.080E-17	N
3062.	211	02200002-	00000000	2906-	3254	755	3.435E-20	N
(unassigned lines)	211	-		2511-	3176	847	1.701E-20	N
	311	-		3157-	3175	4	1.302E-22	N
4223.497	211	10000111-	00000000	4136-	4279	151	2.129E-19	N
4340.	211	00011112-	00000000	4147-	4490	958	4.077E-19	N
4540.	211	01111002-	00000000	4409-	4667	388	6.246E-20	N
(unassigned lines)	211	-		3900-	4667	2116	1.196E-19	N
5987.3255	311	00022002-	00000000	5897-	6078	93	4.622E-22	N
6004.991	211	00022002-	00000000	5891-	6107	142	5.172E-20	N

continued

extrapolation of the calculated values. Transitions for the less abundant species were assumed to have the same halfwidths as the corresponding transitions for the principal isotopic species, $^{16}O_3$. The uncertainty is estimated at 7–10% (Ref. 33) for the principal isotopic species.

Recently Smith *et al.*[35] made measurements of halfwidths of ozone for N_2-, O_2-, and air-broadening. In a comparison, they noted that the calculated values[33] are low by a fairly constant 6% for ν_1 lines. For several ν_3 lines they found the calculations to be only ≈3% low. The better agreement for the ν_3 lines is attributed to the calculations for ν_3 explicitly including the vibrational dependence of the halfwidth (see Ref. 34 for details).

D. N_2O

The line positions and intensities of nitrous oxide in the 894–2630-cm^{-1} region are those of Toth[10,36–39]; the remainder above that region (which date back to studies in the early 1970s) have not changed on the compilation. Below 894 cm^{-1} the ν_2 region has been previ-

Table V, continuation 19

N_2O Molecule: number of lines = 2254

Band Centers	Isotope	Vibrational Band upper	lower	Frequency min	max	number lines	Sum of Intensity
	66	X0-	X0	0-	276	251	7.231E-24
	68	X0-	X0	1-	214	218	3.033E-26
	67	X0-	X0	1-	132	465	4.537E-27
	66	X1-	X1	1-	207	100	3.764E-27
1556.385	66	X1-	X0	1407-	1706	146	6.152E-27
6326.0326	66	a0-	X1	6284-	6410	47	1.129E-28
7882.4248	66	a0-	X0	7664-	8065	157	1.816E-24
7883.7375	68	a0-	X0	7809-	7984	147	6.745E-27
9365.8772	66	a1-	X0	9264-	9469	88	8.626E-27
11564.516	66	b0-	X1	11483-	11617	47	7.798E-27
12969.269	66	b1-	X1	12847-	13011	59	9.418E-26
13120.909	66	b0-	X0	12899-	13166	91	1.946E-22
13122.972	68	b0-	X0	12981-	13165	136	7.921E-25
14488.826	68	b1-	X0	14373-	14520	108	4.960E-26
14506.26	67	b1-	X0	14453-	14537	45	1.831E-26
14525.661	66	b1-	X0	14317-	14558	79	1.218E-23
15828.247	68	b2-	X0	15846-	15849	3	8.884E-29
15902.418	66	b2-	X0	15719-	15928	67	3.782E-25

continued

ously updated.[40] The majority of the new parameters were derived from laboratory measurements of which the uncertainties associated with positions are 0.0001 cm^{-1} or better and the intensities are 2–5%.

Table V lists the N_2O band centers, isotopic species, upper and lower state vibrational states, frequency range of the band, number of lines, and sum of the line intensities. The updated bands (in terms of line positions and intensities) for this edition are indicated by a letter N after the sum of line intensities. The line positions and intensities for a number of transitions in the 10^01–10^00 band of the $^{14}N_2{}^{16}O$ species centered at 2195.9158 cm^{-1} are perturbed and measured values of positions and intensities were inserted in place of the nonperturbed, computed values for those lines. The interacting states are 10^01, 06^00, and 06^20, and only the transitions of the enhanced lines of the 06^00–10^00 and 06^20–10^00 bands were included in the listing. These interactions are very apparent in the ground state bands of these states located in the 3450-cm^{-1} region. However, the positions and intensities of the perturbed transitions given in the present compilation do not consider these interactions and caution should be used for application of those lines. Further work[10] is in progress from which a listing of line positions and intensities covering the 2700–5300-cm^{-1} region will be obtained and, where necessary, measured values will replace computed ones for the perturbed lines.

Updated halfwidths have been added to all the N_2O lines on the database. The values are from the work of Lacome *et al.*[41] which consist of experimental values for N_2- and O_2-broadening from $|m| = 1$ to 49 and theoretical values out to $|m| = 61$. The air-broadened values are given by the formula

$$\gamma_{air} = 0.79\,\gamma_{N2} + 0.21\,\gamma_{O2}. \quad (6)$$

Use of the theoretical values beyond $|m| = 49$ with the experimental values below 49 gives a discontinuity in the halfwidths as a function of $|m|$. The differences between the theoretical and experimental values were calculated and fitted to the formula dif $= a + b|m|$, giving $a = -1.603$, $b = 0.2684$ with the correlation coefficient of the fit being 0.9988. From this linear expression the halfwidths were smoothly continued to $|m| = 61$. Beyond $|m| = 61$ the default value of 0.0686 cm^{-1}/atm was used. The uncertainty in the measured halfwidths is estimated at 5–10% and between 10 and 20% for the scaled theoretical values.

E. CH_4

In the compilation, there are 32 individual bands of methane between 0 and 6107 cm^{-1} with a total integrated absorption of 1.74×10^{-17} $cm^{-1}/(molec \cdot cm^{-2})$. Three isotopes are cataloged: $^{12}CH_4$, $^{13}CH_4$, and $^{12}CH_3D$. The bands fall in five spectral regions.

In the dyad region (1000–1950 cm^{-1}), no changes have been made to the line positions of the two fundamentals of $^{12}CH_4$ and $^{13}CH_4$. However, the line intensities of ν_2 and ν_4 of $^{13}CH_4$ have been lowered by 3% and multiplied by an empirical Herman-Wallis factor pre-

Table V, continuation 20

NO Molecule: number of lines = 7385

Band Centers	Isotope	Vibrational Band upper	lower	Frequency min	max	number lines	Sum of Intensity
	46 X3/2	0-X3/2	0	0-	98	301	1.218E-20
	46 X1/2	0-X1/2	0	0-	99	298	2.222E-20
	46 X3/2	5-X3/2	4	1626-	1856	103	2.685E-33
	46 X1/2	5-X1/2	4	1629-	1855	106	4.988E-33
	46 X3/2	5-X1/2	4	1792-	2020	104	1.739E-36
	46 X1/2	5-X3/2	4	1463-	1692	103	7.974E-37
	46 X3/2	4-X3/2	3	1652-	1886	103	1.324E-29
	46 X3/2	4-X1/2	3	1820-	2051	104	8.734E-33
	46 X1/2	4-X1/2	3	1656-	1885	106	2.466E-29
	46 X1/2	4-X3/2	3	1488-	1720	103	4.003E-33
	46 X3/2	3-X3/2	2	1679-	1915	103	7.034E-26
	46 X1/2	3-X3/2	2	1514-	1748	103	2.164E-29
	46 X3/2	3-X1/2	2	1847-	2081	104	4.720E-29
	46 X1/2	3-X1/2	2	1682-	1914	106	1.312E-25
	46 X3/2	1-X3/2	0	1733-	1974	205	1.743E-18
	56 X3/2	1-X3/2	0	1705-	1938	199	6.683E-21
	48 X3/2	1-X3/2	0	1692-	1921	197	3.674E-21
	46 X1/2	1-X3/2	0	1566-	1805	206	5.530E-22
	56 X1/2	1-X3/2	0	1609-	1769	142	1.972E-24
	48 X1/2	1-X3/2	0	1601-	1751	132	1.045E-24
	46 X3/2	1-X1/2	0	1903-	2142	210	1.205E-21
	56 X3/2	1-X1/2	0	1892-	2061	156	4.307E-24
	48 X3/2	1-X1/2	0	1880-	2039	150	2.289E-24
	46 X1/2	1-X1/2	0	1736-	1972	212	3.258E-18
	56 X1/2	1-X1/2	0	1708-	1936	202	1.248E-20
	48 X1/2	1-X1/2	0	1695-	1919	200	6.861E-21
	46 X3/2	2-X3/2	1	1706-	1944	205	3.767E-22
	46 X1/2	2-X3/2	1	1540-	1777	206	1.175E-25
	46 X3/2	2-X1/2	1	1875-	2112	208	2.562E-25
	46 X1/2	2-X1/2	1	1709-	1943	212	7.034E-22
	46 X3/2	6-X3/2	4	3339-	3569	103	1.155E-34
	46 X3/2	6-X1/2	4	3505-	3733	104	7.217E-38
	46 X1/2	6-X3/2	4	3177-	3416	103	3.555E-38
	46 X1/2	6-X1/2	4	3344-	3569	106	2.147E-34
	46 X3/2	5-X3/2	3	3394-	3626	103	4.511E-31
	46 X3/2	5-X1/2	3	3561-	3791	104	2.868E-34
	46 X1/2	5-X3/2	3	3231-	3472	103	1.411E-34
	46 X1/2	5-X1/2	3	3398-	3626	106	8.394E-31
	46 X3/2	4-X3/2	2	3449-	3683	103	1.896E-27
	46 X3/2	4-X1/2	2	3617-	3849	104	1.228E-30
	46 X1/2	4-X3/2	2	3285-	3528	103	6.036E-31
	46 X1/2	4-X1/2	2	3453-	3683	106	3.537E-27
	46 X3/2	3-X3/2	1	3504-	3741	103	4.848E-24
	46 X3/2	3-X1/2	1	3673-	3908	104	3.194E-27
	46 X1/2	3-X3/2	1	3339-	3584	103	1.570E-27
	46 X1/2	3-X1/2	1	3508-	3741	106	9.054E-24
	46 X3/2	2-X3/2	0	3559-	3798	206	2.814E-20
	46 X3/2	2-X1/2	0	3729-	3967	208	1.879E-23
	46 X1/2	2-X3/2	0	3392-	3641	206	9.235E-24
	46 X1/2	2-X1/2	0	3563-	3798	212	5.262E-20

continued

Table V, continuation 21

SO$_2$ Molecule: number of lines = 23659

Band Centers	Isotope	Vibrational Band upper	lower	Frequency min	max	number lines	Sum of Intensity	
	626	000-	000	0-	257	9622	2.583E-18	N
517.75	626	010-	000	433-	617	3326	3.899E-18	
1151.7135	626	100-	000	1047-	1262	5812	3.519E-18	
1362.0295	626	001-	000	1316-	1394	2075	3.080E-17	
2475.8300	646	101-	000	2463-	2497	287	6.027E-21	
2492.4438	626	111-	010	2463-	2516	654	2.110E-20	
2499.8701	626	101-	000	2463-	2527	1883	3.954E-19	

NO$_2$ Molecule: number of lines = 20067

Band Centers	Isotope	Vibrational Band upper	lower	Frequency min	max	number lines	Sum of Intensity	
	646	000-	000	1-	100	6360	2.165E-19	N
749.6537	646	010-	000	609-	987	4756	5.380E-19	N
1616.8520	646	001-	000	1550-	1657	3276	6.113E-17	
2805.5122	646	120-	000	2860-	2926	57	3.327E-22	N
2898.1930	646	111-	010	2832-	2918	1829	1.056E-19	N
2906.0697	646	101-	000	2828-	2939	3789	2.882E-18	N

NH$_3$ Molecule: number of lines = 5817

Band Centers	Isotope	Vibrational Band upper	lower	Frequency min	max	number lines	Sum of Intensity	
	4111	0000 -	0000	19-	415	441	1.773E-17	
	5111	0000 -	0000	19-	408	362	6.563E-20	
	4111	0000a-	0000s	0-	1	49	9.081E-25	
	5111	0000a-	0000s	0-	1	15	4.516E-27	
	4111	0100a-	0100s	12-	477	394	2.172E-19	
	4111	0100s-	0100a	4-	368	199	7.341E-20	
629.418	4111	0200s-	0100a	309-	1054	343	1.468E-19	
927.685	5111	0100s-	0000a	637-	1235	293	3.981E-20	
931.642	4111	0100 -	0000a	560-	1293	459	1.079E-17	N
949.656	4111	0200a-	0100s	630-	1244	312	8.784E-20	
962.879	5111	0100a-	0000s	676-	1244	291	3.987E-20	
968.122	4111	0100 -	0000s	612-	1301	460	1.123E-17	N
1596.675	4111	0200s-	0000a	1239-	1967	308	2.097E-20	
1629.991	4111	0001 -	0000s	1204-	1998	793	2.053E-18	N
1630.339	4111	0001 -	0000a	1229-	2056	793	2.047E-18	N
1882.175	4111	0200a-	0000s	1564-	2154	305	2.071E-20	

continued

viously applied to the bands of the main isotope.[3] The accuracies of the positions range from 0.0005 to 0.005 cm^{-1} and intensities from 4% to 15%. The best accuracies are associated with the allowed lines of the ν_4 band of the main isotope. While several hot bands (such as $\nu_2 + \nu_4 - \nu_2$ and $2\nu_4 - \nu_4$) are needed to complete the compilation, only the prediction of the $\nu_3 - \nu_4$ hot band of $^{12}CH_4$ has been included.[42] However, the ν_3, ν_5, and ν_6 fundamentals of CH_3D (Refs. 43–45) from the GEISA compilation[5] have been added; intensities have been scaled by the isotopic abundance ratio of 6.0×10^{-4}. Accuracies of the CH_3D positions are between 0.002 and 0.01 cm^{-1}. Because the CH_3D bands are perturbed, some predicted relative intensities may be in error by substantial amounts. The ν_2 fundamental of CH_3D at 2200 cm^{-1} has not been added, but a nearby overtone band, $2\nu_6$ (Ref. 46), has been taken from the GEISA compilation.[5]

In the pentad region, the compilation has been extended to cover an additional 180 cm^{-1}, from 2255 to 3255 cm^{-1}, by combining the recent pentad prediction of the five bands (ν_3, ν_1, $2\nu_4$, $2\nu_2$, and $\nu_2 + \nu_4$) of the main

Table V, continuation 22

HNO$_3$ Molecule: number of lines = 35988

Band Centers	Isotope	Vibrational Band upper	lower	Frequency min	max	number lines	Sum of Intensity	
	146	Ground-	Ground	0-	43	4182	5.819E-19	
879.1082	146	V5-	Ground	840-	918	8313	1.261E-17	N
896.4187	146	2V9-	Ground	852-	920	7250	9.843E-18	N
	146	V5+V9-	V9	847-	905	3971	1.216E-18	N
	146	3V9-	V9	845-	909	4780	2.030E-18	N
1709.5676	146	V2-	Ground	1670-	1750	7492	2.014E-17	

OH Molecule: number of lines = 8676

Band Centers	Isotope	Vibrational Band upper		lower		Frequency min	max	number lines	Sum of Intensity	
	61	X3/2	0-	X3/2	0	0-	331	94	2.896E-17	N
	81	X3/2	0-	X3/2	0	0-	7	40	8.635E-26	
	62	X3/2	0-	X3/2	0	0-	2	60	8.245E-28	
	61	X1/2	0-	X3/2	0	31-	311	116	1.044E-18	N
	61	X1/2	0-	X1/2	0	0-	327	89	1.420E-17	N
	81	X1/2	0-	X1/2	0	0-	3	25	6.290E-27	
	62	X1/2	0-	X1/2	0	0-	1	30	2.467E-28	
	61	X3/2	9-	X3/2	8	1709-	2418	86	4.448E-68	
	61	X3/2	9-	X1/2	8	1287-	2139	88	1.335E-70	
	61	X1/2	9-	X3/2	8	2082-	2812	86	2.297E-70	
	61	X1/2	9-	X1/2	8	1667-	2417	92	2.001E-68	
	61	X3/2	8-	X3/2	7	1873-	2625	86	2.577E-63	
	61	X3/2	8-	X1/2	7	1429-	2319	88	8.217E-66	
	61	X1/2	8-	X3/2	7	2268-	3048	86	1.262E-65	
	61	X1/2	8-	X1/2	7	1832-	2625	92	1.164E-63	
	61	X3/2	7-	X3/2	6	2027-	2823	86	2.660E-58	
	61	X3/2	7-	X1/2	6	1560-	2492	88	8.362E-61	
	61	X1/2	7-	X3/2	6	2443-	3268	86	1.024E-60	
	61	X1/2	7-	X1/2	6	1985-	2823	92	1.222E-58	
	61	X3/2	6-	X3/2	5	2175-	3014	86	4.485E-53	
	61	X3/2	6-	X1/2	5	1687-	2661	88	9.619E-56	
	61	X1/2	6-	X3/2	5	2611-	3482	86	9.424E-56	
	61	X1/2	6-	X1/2	5	2132-	3016	92	2.157E-53	
	61	X3/2	5-	X3/2	4	2320-	3200	86	3.803E-47	
	61	X3/2	5-	X1/2	4	1810-	2826	88	6.344E-50	
	61	X1/2	5-	X3/2	4	2776-	3690	86	3.718E-49	
	61	X1/2	5-	X1/2	4	2276-	3204	92	1.754E-47	
	61	X3/2	4-	X3/2	3	2463-	3384	86	1.737E-40	
	61	X3/2	4-	X1/2	3	1931-	2990	88	6.215E-43	
	61	X1/2	4-	X3/2	3	2937-	3895	86	2.293E-42	
	61	X1/2	4-	X1/2	3	2417-	3389	92	7.449E-41	
	61	X3/2	3-	X3/2	2	2605-	3567	86	1.737E-33	
	61	X3/2	3-	X1/2	2	2052-	3154	88	7.634E-36	
	61	X1/2	3-	X3/2	2	3098-	4099	86	2.288E-35	
	61	X1/2	3-	X1/2	2	2557-	3573	92	7.339E-34	
	61	X3/2	2-	X3/2	1	2747-	3750	86	2.815E-26	
	61	X3/2	2-	X1/2	1	2172-	3319	88	1.375E-28	
	61	X1/2	2-	X3/2	1	3259-	4303	86	3.708E-28	
	61	X1/2	2-	X1/2	1	2698-	3757	92	1.184E-26	
	61	X3/2	1-	X3/2	0	2890-	3934	86	6.744E-19	
	61	X3/2	1-	X1/2	0	2293-	3486	88	3.560E-21	

continued

Table V, continuation 23

61	X1/2	1-X3/2	0	3422-	4509	86	8.993E-21
61	X1/2	1-X1/2	0	2839-	3943	92	2.830E-19
61	X3/2	9-X3/2	7	3947-	4761	86	2.544E-63
61	X3/2	9-X1/2	7	3503-	4538	88	9.079E-66
61	X1/2	9-X3/2	7	4320-	5080	86	2.080E-65
61	X1/2	9-X1/2	7	3883-	4759	92	1.109E-63
61	X3/2	8-X3/2	6	4287-	5126	86	6.896E-58
61	X3/2	8-X1/2	6	3821-	4889	88	2.640E-60
61	X1/2	8-X3/2	6	4682-	5484	86	5.851E-60
61	X1/2	8-X1/2	6	4224-	5125	92	2.990E-58
61	X3/2	7-X3/2	5	4611-	5479	86	3.684E-52
61	X3/2	7-X1/2	5	4123-	5229	88	1.504E-54
61	X1/2	7-X3/2	5	5027-	5874	86	3.260E-54
61	X1/2	7-X1/2	5	4547-	5478	92	1.590E-52
61	X3/2	6-X3/2	4	4926-	5824	86	3.879E-46
61	X3/2	6-X1/2	4	4416-	5560	88	1.691E-48
61	X1/2	6-X3/2	4	5361-	6253	86	3.592E-48
61	X1/2	6-X1/2	4	4861-	5823	92	1.663E-46
61	X3/2	5-X3/2	3	5234-	6165	86	8.053E-40
61	X3/2	5-X1/2	3	4703-	5888	88	3.741E-42
61	X1/2	5-X3/2	3	5689-	6624	86	7.826E-42
61	X1/2	5-X1/2	3	5168-	6165	92	3.448E-40
61	X3/2	4-X3/2	2	5538-	6506	86	3.229E-33
61	X3/2	4-X1/2	2	4986-	6215	88	1.590E-35
61	X1/2	4-X3/2	2	6013-	6991	86	3.286E-35
61	X1/2	4-X1/2	2	5472-	6505	92	1.376E-33
61	X3/2	3-X3/2	1	5842-	6846	86	2.376E-26
61	X3/2	3-X1/2	1	5268-	6542	88	1.242E-28
61	X1/2	3-X3/2	1	6336-	7358	86	2.528E-28
61	X1/2	3-X1/2	1	5774-	6845	92	1.009E-26
61	X3/2	2-X3/2	0	6148-	7189	86	2.513E-19
61	X3/2	2-X1/2	0	5552-	6872	88	1.388E-21
61	X1/2	2-X3/2	0	6661-	7726	86	2.800E-21
61	X1/2	2-X1/2	0	6078-	7189	92	1.063E-19
61	X3/2	9-X3/2	6	6361-	7319	86	1.873E-58
61	X3/2	9-X1/2	6	5895-	7116	88	7.081E-61
61	X1/2	9-X3/2	6	6734-	7582	86	1.477E-60
61	X1/2	9-X1/2	6	6275-	7316	92	8.151E-59
61	X3/2	8-X3/2	5	6871-	7845	86	6.739E-53
61	X3/2	8-X1/2	5	6384-	7633	88	2.731E-55
61	X1/2	8-X3/2	5	7266-	8136	86	5.603E-55
61	X1/2	8-X1/2	5	6787-	7842	92	2.918E-53
61	X3/2	7-X3/2	4	7361-	8356	86	4.949E-47
61	X3/2	7-X1/2	4	6852-	8136	88	2.141E-49
61	X1/2	7-X3/2	4	7777-	8674	86	4.338E-49
61	X1/2	7-X1/2	4	7277-	8354	92	2.040E-47
61	X3/2	6-X3/2	3	7839-	8859	86	7.477E-41
61	X3/2	6-X1/2	3	7308-	8630	88	3.443E-43
61	X1/2	6-X3/2	3	8275-	9204	86	6.896E-43
61	X1/2	6-X1/2	3	7754-	8857	92	3.207E-41
61	X3/2	5-X3/2	2	8309-	9358	86	2.255E-34
61	X3/2	5-X1/2	2	7757-	9120	88	1.100E-36
61	X1/2	5-X3/2	2	8764-	9730	86	2.186E-36
61	X1/2	5-X1/2	2	8223-	9356	92	9.624E-35
61	X3/2	4-X3/2	1	8776-	9857	86	1.218E-27
61	X3/2	4-X1/2	1	8202-	9610	88	6.292E-30
61	X1/2	4-X3/2	1	9250-	9985	60	1.228E-29

continued

Table V, continuation 24

	61	X1/2	4-X1/2	1	8688- 9856	92	5.178E-28
	61	X3/2	3-X3/2	0	9244- 9989	34	3.952E-22
	61	X3/2	3-X1/2	0	8648- 9997	70	1.659E-23
	61	X1/2	3-X3/2	0	9737- 9981	10	1.243E-28
	61	X1/2	3-X1/2	0	9154- 9998	38	2.522E-22

HF Molecule: number of lines = 62

Band Centers	Isotope	Vibrational Band upper	lower	Frequency min	max	number lines	Sum of Intensity
	19	0-	0	41-	589	15	5.704E-17
3961.4429	19	1-	0	3381-	4339	25	1.547E-17
7750.7949	19	2-	0	7143-	7993	22	4.962E-19

HCl Molecule: number of lines = 200

Band Centers	Isotope	Vibrational Band upper	lower	Frequency min	max	number lines	Sum of Intensity
	15	0-	0	20-	383	19	8.068E-18
	17	0-	0	20-	383	19	2.620E-18
2883.8850	17	1-	0	2486-	3136	33	1.472E-18
2885.9765	15	1-	0	2459-	3139	34	4.528E-18
5663.9276	17	2-	0	5303-	5824	27	3.480E-20
5667.9832	15	2-	0	5271-	5830	29	1.071E-19
8340.9407	17	3-	0	8124-	8449	18	2.279E-22
8346.7771	15	3-	0	8058-	8455	21	7.068E-22

HBr Molecule: number of lines = 256

Band Centers	Isotope	Vibrational Band upper	lower	Frequency min	max	number lines	Sum of Intensity
	19	0-	0	16-	339	21	2.398E-18
	11	0-	0	16-	339	21	2.346E-18
	19	1-	1	64-	130	5	6.849E-24
	11	1-	1	64-	130	5	6.713E-24
2558.5308	11	1-	0	2195-	2773	36	7.232E-19
2558.9105	19	1-	0	2195-	2773	36	7.392E-19
5026.6005	11	2-	0	4712-	5160	28	7.549E-21
5027.3408	19	2-	0	4713-	5161	28	7.715E-21
7404.1928	11	3-	0	7204-	7495	20	1.929E-22
7405.2610	19	3-	0	7205-	7496	20	1.971E-22
9690.9914	11	4-	0	9506-	9758	18	9.473E-23
9692.3579	19	4-	0	9507-	9759	18	9.682E-23

HI Molecule: number of lines = 145

Band Centers	Isotope	Vibrational Band upper	lower	Frequency min	max	number lines	Sum of Intensity
	17	0-	0	12-	286	23	1.067E-18
	17	1-	1	49-	137	8	1.798E-23
2229.5817	17	1-	0	2117-	2398	26	1.758E-20
4379.2261	17	2-	0	4117-	4489	32	6.330E-21
6448.0348	17	3-	0	6176-	6521	30	3.430E-21
8434.7076	17	4-	0	8190-	8488	26	5.932E-22

continued

Table V, continuation 25

ClO Molecule: number of lines = 6020

Band Centers	Isotope	Vibrational Band upper	lower	Frequency min	max	number lines	Sum of Intensity
	56	X3/2	0-X3/2 0	3-	100	1215	4.815E-19
	76	X3/2	0-X3/2 0	3-	100	1232	1.542E-19
	56	X1/2	0-X1/2 0	0-	100	1360	1.015E-19
	76	X1/2	0-X1/2 0	0-	99	1375	3.251E-20
835.4800	76	X3/2	1-X3/2 0	763-	883	218	9.825E-20
842.5540	56	X3/2	1-X3/2 0	769-	891	224	3.062E-19
	56	X1/2	1-X1/2 0	769-	887	212	6.363E-20
	76	X1/2	1-X1/2 0	770-	877	184	2.036E-20

OCS Molecule: number of lines = 737

Band Centers	Isotope	Vibrational Band upper	lower	Frequency min	max	number lines	Sum of Intensity
	622	0000-	0000	0-	40	99	8.034E-20
	624	0000-	0000	0-	40	99	3.647E-21
	632	0000-	0000	0-	38	93	9.407E-22
	822	0000-	0000	0-	32	84	1.596E-22
858.9669	622	1000-	0000	817-	891	181	1.098E-18
2062.2	622	0001-	0000	2016-	2089	181	7.881E-17

H_2CO Molecule: number of lines = 2702

Band Centers	Isotope	Vibrational Band upper	lower	Frequency min	max	number lines	Sum of Intensity	
	126	000000-	000000	0-	100	611	3.265E-18	N
	136	000000-	000000	0-	73	563	5.633E-20	
	128	000000-	000000	0-	48	367	6.941E-21	
2500.	126	000002-	000000	2743-	2812	5	4.548E-20	
2655.	126	001100-	000000	2734-	2735	1	5.890E-21	
2719.156	126	001001-	000000	2700-	2879	105	1.386E-18	
2782.457	126	100000-	000000	2723-	2843	424	8.288E-18	
2843.326	126	000010-	000000	2703-	2982	595	9.742E-18	
2905.	126	010100-	000000	2734-	2999	28	3.813E-19	
3000.066	126	010001-	000000	2896-	2957	3	8.550E-20	

HOCl Molecule: number of lines = 15565

Band Centers	Isotope	Vibrational Band upper	lower	Frequency min	max	number lines	Sum of Intensity	
	165	000-	000	0-	333	3919	1.502E-17	N
	167	000-	000	0-	334	3923	4.801E-18	N
1238.1208	167	010-	000	1179-	1303	1240	2.917E-18	
1238.6242	165	010-	000	1174-	1311	1463	8.962E-18	
3609.4801	165	100-	000	3400-	3800	2675	3.044E-18	
3609.4851	167	100-	000	3400-	3800	2345	9.769E-19	

continued

isotope[47,48] with old[49] and new[50] measurements. In this revision, all the positions of Refs. 47 and 48 have been multiplied by 0.999999765 to conform with the *P*7 line calibration standard (2947.91206 cm^{-1}, Ref. 51). In addition, detailed comparisons with laboratory spectra from the Fourier transform spectrometer at the National Solar Observatory on Kitt Peak[50] have been used to guide the modification of some of the positions and intensities in the compilation. Calculated intensities of the pentad region have been used if

Table V, continuation 26

N_2 Molecule: number of lines = 117

Band Centers	Isotope	Vibrational Band upper	lower	Frequency min	max	number lines	Sum of Intensity	
2329.9168	44	1-	0	2001-	2620	117	6.392E-27	

HCN Molecule: number of lines = 772

Band Centers	Isotope	Vibrational Band upper	lower	Frequency min	max	number lines	Sum of Intensity	
	124	0000-	0000	2-	132	47	1.026E-17	
	134	0000-	0000	2-	98	34	1.223E-19	
	125	0000-	0000	2-	101	35	4.036E-20	
697.957	124	0200-	0110	587-	823	119	2.498E-19	
713.076	124	0220-	0110	595-	851	232	1.033E-18	
713.459	124	0110-	0000	579-	844	134	8.230E-18	
1426.535	124	0200-	0000	1298-	1537	81	1.399E-18	
3311.4772	124	0001-	0000	3158-	3422	90	9.516E-18	

CH_3Cl Molecule: number of lines = 6687

Band Centers	Isotope	Vibrational Band upper	lower	Frequency min	max	number lines	Sum of Intensity	
2967.745	217	V1-	Ground	2965-	2969	229	4.919E-20	
2967.777	215	V1-	Ground	2965-	2969	255	1.543E-19	
3039.1761	217	V4-	Ground	2986-	3162	1260	2.016E-19	
3039.2864	215	V4-	Ground	2978-	3173	1844	5.878E-19	
3041.8005	217	3V6-	Ground	2916-	3128	1221	1.928E-19	
3042.8736	215	3V6-	Ground	2907-	3157	1878	6.658E-19	

H_2O_2 Molecule: number of lines = 3272

Band Centers	Isotope	Vibrational Band upper	lower	Frequency min	max	number lines	Sum of Intensity	
	1661	000000-	000000	0-	100	883	2.886E-18	N
1269.136	1661	000001-	000000	1186-	1350	2389	1.284E-17	

C_2H_2 Molecule: number of lines = 1139

Band Centers	Isotope	Vibrational Band upper	lower	Frequency min	max	number lines	Sum of Intensity	
719.9658	1221	00000200-	00000111	640-	805	93	9.430E-19	N
728.8574	1221	00011110-	00011001	638-	811	198	1.439E-18	N
729.1365	1221	00000222-	00000111	655-	820	187	1.119E-18	N
729.1553	1221	00000111-	00000000	646-	811	182	2.383E-17	N
731.1074	1221	00011112-	00011001	650-	822	191	1.355E-18	N
3281.9020	1221	01011110-	00000000	3151-	3387	101	5.004E-18	N
3284.1904	1231	00100000-	00000000	3178-	3375	86	1.835E-19	N
3294.8406	1221	00100000-	00000000	3162-	3398	101	4.420E-18	N

continued

Table V, continuation 27

C H Molecule: number of lines = 4328
 2 6

Band Centers	Isotope	Vibrational Band upper	lower	Frequency min	max	number lines	Sum of Intensity
821.7234	1221	V9-	Ground	720-	933	4328	1.456E-18

PH Molecule: number of lines = 2886
 3

Band Centers	Isotope	Vibrational Band upper	lower	Frequency min	max	number lines	Sum of Intensity
992.1301	1111	0100 -	0000	708-	1211	972	3.306E-18

Notes: Sum of Intensities reflect sum of lines on compilation
"N" denotes totally updated or new bands for this edition
Units for band centers and range are cm^{-1};
intensity sum in $cm^{-1}/(molec \cdot cm^{-2})$ @296K.

Table VI. Species Included in Cross-Sectional File

Species		# cross sections	Frequency cm^{-1} Minimum	Maximum
$ClONO_2$		5020	765.002	819.998
HNO_4		5476	770.007	829.999
$CHCl_2F$	(CFC21)	5020	785.000	839.995
CCl_4		1826	786.001	805.998
$CFCl_3$	(CFC11)	2738	830.009	859.999
CF_2Cl_2	(CFC12)	7301	860.008	939.996
$C_2Cl_2F_4$	(CFC114)	12320	1025.009	1159.992
$CHCl_2F$	(CFC21)	4563	1050.004	1099.992
$CFCl_3$	(CFC11)	3651	1060.004	1099.998
CF_2Cl_2	(CFC12)	10039	1070.005	1179.994
$C_2Cl_3F_3$	(CFC113)	12777	1090.008	1229.998
$C_2Cl_2F_4$	(CFC114)	11771	1160.025	1288.992
N_2O_5		4647	1225.001	1265.000
HNO_3		7301	1270.004	1349.993
$ClONO_2$		3650	1270.007	1309.991
CF_4		1095	1275.003	1286.990
N_2O_5		11616	1680.003	1780.000

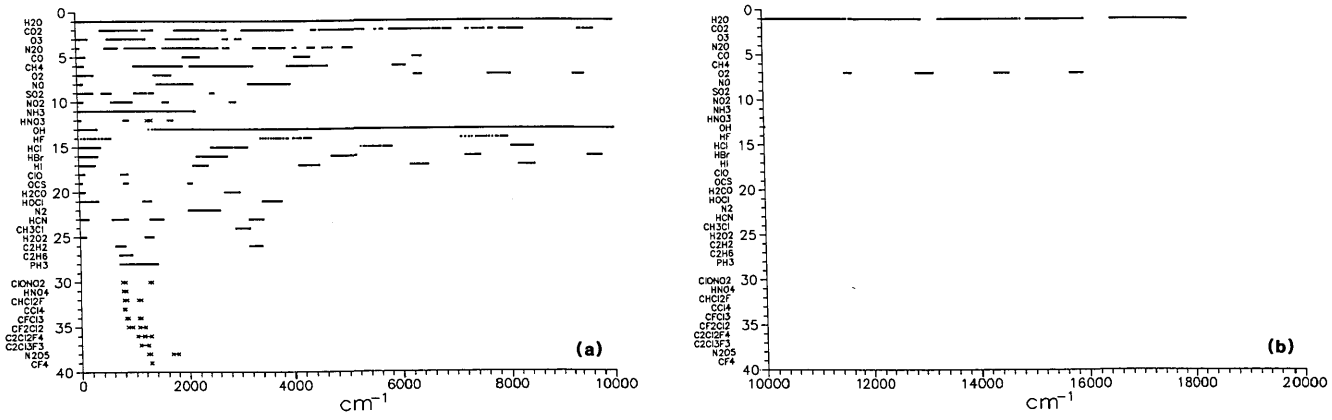

Fig. 2. Spectral regions covered for each molecule in HITRAN: (a) 0–10000 cm^{-1}; (b) 10,000–20,000 cm^{-1}.

they differ from the measured intensities by no more than 10%. New experimental line intensities[50] have been used in most of the 2250–2385-cm^{-1} region and the 3200–3250-cm^{-1} region. Finally, the CH_3D parameters appearing in this region on the 1982 compilation[3] have been replaced with the CH_3D list taken from the 1984 GEISA compilation.[5] The rotational quantum numbers follow two different conventions. The pentad calculation uses three quantum numbers, J, C, and N (see Refs. 47 and 48) while the older portions of the compilation use four quantum numbers, J, R, C, and N (see Refs. 3 and 49).

The parameters in the pentad region are, for the most part, still based on an experimental line list to which assignments of the three isotopes have been ascribed. The intensities[49] between 2385 and 3200 cm^{-1} were generally measured at 0.02-cm^{-1} resolution using a grating spectrometer, with gas samples whose temperatures differed by as much as 4° from scan to scan. However, the intensities were never normalized to 296 K because most lines were unassigned at the time of the original work.[3,49] Later analysis indicated tentative assignments for many of the absorptions, but some lines may be wrongly assigned, or some isotopic lines (and bands) may be missing, or the observed absorption may actually arise from more transitions than are currently ascribed. Thus the sums of intensities given in Table V in many cases do not reflect the integrated band intensities. These parameters do reproduce laboratory spectra recorded at room temperature[50] and at 0.01-cm^{-1} resolution, but extrapolation of weak lines to much different temperatures may produce large errors. While some of the line intensities are good to 2% or better (allowed P-branch lines of the ν_3 band of the main isotope), lines weaker than 10^{-23} $cm^{-1}/(molec \cdot cm^{-2})$ are often good to only 15% and very weak lines may be in error by as much as 50%. Similarly, accuracies of positions range from 0.0006 to 0.005 cm^{-1}. Much work is needed to model the measurements and provide a complete and accurate prediction of the region.

The octad region from 3500 to 5000 cm^{-1} is also based on measurements with tentative assignments given up to $J = 12$ of the main isotope.[50,52,53] However, only three bands ($\nu_2 + \nu_4$, $\nu_3 + \nu_4$, and $\nu_2 + \nu_3$) of a possible eight are indicated at present and, for the 4166–4666-cm^{-1} region, no lines weaker than 2×10^{-23} $cm^{-1}/(molec \cdot cm^{-2})$ are given. For the 1986 edition, experimental positions and intensities[50,53] in the region of $3\nu_4$ and $2\nu_4 + \nu_2$ between 3750 and 4136 cm^{-1} have been added without assignments. This change increases the total CH_4 absorption in this region of the compilation by ~5%. Because of new calibration standards,[54] all positions appearing in the 1982 version[3] between 4136 and 4666 cm^{-1} have been lowered by 0.0006 cm^{-1}.

The region between 5000 and 6500 cm^{-1} contains up to 40 states, a dozen of which probably give rise to significant absorption in atmospheric spectra. At present, however, only an older prediction of one band, $2\nu_3$, is included and only to modest values of J. For the 1986 update, an error in band intensity (that has existed since the first edition[1]) has been corrected by multiplying intensities by 2.5 to conform to existing measurements.[55] The parameters of the $^{13}CH_4$ $2\nu_3$ band[56] have also been added using isotopically scaled intensities of the $^{12}CH_4$ prediction. The accuracies of the parameters are thought to be 0.005–0.020 cm^{-1} for positions and 5–20% for intensities.

As in previous editions of the compilation, air-broadened halfwidths were determined from the calculated O_2- and N_2-broadened halfwidths of Tejwani and Fox[57] corrected to 296 K. In the future this parameter will be reevaluated in light of the measurements of Varanasi *et al.*[58,59] and Devi *et al.*[60,61]

F. O_2

The only update for oxygen on this edition has been the introduction of the zero frequency lines. These parameters have the frequency set to a synthetic frequency of $g \cdot J$ (where g is the degeneracy of the level) and come directly from Ref. 6. The transitions play an important role in the millimeter-wavelength soundings of the atmosphere. The halfwidths used for these lines are the same as previously employed for the 60-GHz transitions.

G. SO_2

The pure rotation lines of sulfur dioxide have been updated with the data of Poynter and Pickett.[6] The data are a refit of the pure rotational spectrum for all lines of J up to 74 and K up to 28. The Hamiltonian constants were obtained by fitting to the experimental measurements of Lovas[62] with additional selected lines taken from Carlotti *et al.*[63] The dipole moment was taken from the work of Patel *et al.*[64] The line intensities are accurate to a few percent and the line positions are accurate to ±0.001 cm^{-1} or better. The error estimate is given in IER. As before, a constant value of 0.11 cm^{-1}/atm has been adopted for the air-broadened halfwidth.

H. NO_2

The positions and intensities of the nitrogen dioxide lines absorbing in the 6.2-, 3.4-, and 13.3-μm regions have been calculated using a theoretical model taking into account when necessary the Coriolis interaction affecting the rovibrational levels.

In the 6.2-μm region, the main absorbing band is ν_3 and the $K_a = 4, 5, 6$ subbands were correctly reproduced only because the strong Coriolis interaction between the rotational levels of (020) and (001) was taken into account.[65] The line intensities of the ν_3 band were calculated using a pure transition moment operator for this band; in fact the rotational corrections which appear in the transformed transition moment operator and which represent the effect of the vibration–rotation interactions on line intensities were not determined from the set of experimental intensities.[66] These corrections seem to be negligible for medium N and K_a values but they could have an influence for high N and K_a values. Together with the ν_3 band, the hot

band $\nu_2 + \nu_3 - \nu_2$ absorbing in the same spectral region was calculated. The accuracy of the line positions is believed to be on the average 0.003 cm^{-1}. The line intensities are known with a relative precision varying from 5% for low N and K_a values to 20% for high N and K_a values. The ν_3 band was not updated on the present compilation, but the improvements indicated in this paragraph can be obtained from the authors prior to the next edition of HITRAN.

In the 3.4-μm region, the NO_2 absorption is about 20 times weaker than the absorption in the 6.2-μm region, but the former region is of atmospheric interest because it corresponds to a relatively clear transmission window usable for atmospheric measurements from the ground. The main band of nitrogen dioxide absorbing around 3.4 μm is the $\nu_1 + \nu_3$ band and, as for the ν_3 band, the line positions of this combination band have been calculated taking into account the strong Coriolis interaction affecting the rotational levels of the (120) and (101) vibrational states.[67] Since a large set of precise individual line intensities was available for the $\nu_1 + \nu_3$ band,[68] it has been possible to determine through a least-squares fit the rotational expansion of the transformed transition moment operator of this combination band. Finally, this transition moment operator together with the rotational and spin-rotation constants has been used to generate the absorption lines of the $\nu_1 + \nu_3$ and $\nu_1 + 2\nu_2$ bands of NO_2. Moreover, the hot band $\nu_1 + \nu_2 + \nu_3 - \nu_2$ absorbing in the same spectral region has been computed.[67] The accuracy of line positions is believed to be on the average 0.0015 cm^{-1}, the relative accuracy of line intensities varying from 3 to 12%.

The main band absorbing in the 13.3-μm region is the ν_2 band. Diode laser spectra covering selected portions of this band were used to determine the rotational and spin-rotation constants.[69] Line intensities were also measured leading to the determination of the rotational expansion of the transformed transition moment operator of this band.[70] Finally, the spectrum of the ν_2 band of NO_2 was computed; the accuracy of line positions is believed to be 0.002 cm^{-1} for low and medium K_a values, deteriorating for $K_a > 8$. The relative accuracy of the line intensities varies from 5 to 15%.

For all calculations which have been performed, the spin-rotation interaction has been treated using a perturbation method and it should be emphasized that for a few spin-rotation resonating levels the calculation is less precise, leading to positions whose accuracy is worse than the average values quoted here.

In this edition, parameters for the pure rotation band of nitrogen dioxide were added from Ref. 6. The spectrum was determined by a full diagonalization of the Hamiltonian. The data used in the fit were from Bowman and DeLucia.[71] The line intensities have an uncertainty of 2–3%. The accuracy of the line positions is J dependent and generally better than 0.00005 cm^{-1} with a few of the lines having an uncertainty of 0.0003 cm^{-1}. The accuracy of the line positions is given for each line in IER. A constant air-broadened halfwidth of 0.062 cm^{-1}/atm has been assumed for the pure rotation band.

I. NH_3

Two updates of ammonia parameters have been made for this edition. The ν_2 lines of the principal isotope have improved positions, taken from the work of Poynter and Margolis.[72] The ν_4 band has been replaced with the latest parameters from GEISA.[5] An effort was also made to standardize the vibrational notation for all ammonia transitions on this edition.

J. HNO_3

For this edition, the 11-μm bands have been significantly updated. Whereas on previous issues of the database this region was represented by a narrow spectral extent taken from diode laser measurements without lower state energy values, the new database has a broader coverage from 840 to 920 cm^{-1}. The calculations of the parameters are based on studies of laboratory data.[73] The bands now represented are the ν_5 and $2\nu_9$ bands, with approximated hot bands, $\nu_5 + \nu_9 - \nu_9$ and $3\nu_9 - \nu_9$. A few lines belonging to multiplets that cannot be resolved have been coalesced in the same manner as on previous editions, i.e., pairs with the same frequency and intensity have had their intensities added. The coalesced lines are indicated on the database by the omission of the K_a quantum number which allows an unambiguous regeneration of the multiplet if desired for theoretical purposes. Synthetic spectra using these new parameters have been calculated and show very good agreement with recent stratospheric balloon observations.[74] Discrepancies still exist in the region between the band centers of ν_5 and $2\nu_9$; these features will be improved in the future as the resonances of these two bands are adequately represented.

For this edition, the artificial set of lines representing the Q and R branches of the ν_3 band at 1326 cm^{-1} has been removed from the main body of the database, and this band is now included in the cross-sectional file. It is expected that a discrete line parameter formulation for this region will be available for the next update.[75]

The ν_2 band has not been updated for this edition, but much improved parameters exist[76] and will be incorporated in the future. It should be noted that, although the relative intensities of the lines of this band are reasonable, the absolute intensities are too low by approximately a factor of 2.

K. OH

The microwave data for the hydroxyl radical for the ground $^2\pi_{3/2}$ and $^2\pi_{1/2}$ states have been updated. The data are from the JPL catalog[6] and were determined in the same manner as the previous data for this band[4] except that the calculations were extended up to 300 cm^{-1}. As in previous editions, a constant halfwidth of 0.083 cm^{-1}/atm was assumed for the lines. The reported intensities are accurate to a few percent. The accuracy of the line positions is generally better than 0.005 cm^{-1} and shows a dependence on the rotational quantum number.

L. HF

The halfwidths of hydrogen fluoride were updated using the values of Thompson *et al.*[77] The measurements include values for the $P3$ through the $R3$ lines. The uncertainty of the measurements is estimated at 15%. Beyond the observations the previously assumed values were used. More recent measurements[78] of intensities and air- and self-broadened halfwidths will be incorporated in the next edition.

M. HCl

The air-broadened halfwidths for hydrogen chloride have been updated with the measurements of Ballard *et al.*[79] These measurements yield values for the $P(1)$ through $P(8)$ lines, and for the $R(0)$ through $R(7)$ lines and have an estimated uncertainty of 5–15%. The new halfwidths[78] have been applied to all bands and isotopes of HCl on the compilation; beyond the measurements the previous values have been retained. Similar to HF, the intensities and air- and self-broadened halfwidths will be updated[79,80] in the next edition.

N. H_2CO

The pure rotation band of the principal isotopic species of formaldehyde has been updated with data from the JPL catalog.[6] The Hamiltonian formulation of Kirchhoff[81] was used to evaluate the rotational and centrifugal distortion constants. An expanded data set was used in the fit and is given in Ref. 6. The line positions are accurate to 0.003 cm^{-1} for the high wavenumber lines and improves to 0.00002 cm^{-1} or better for low (<1-cm^{-1}) wavenumber transitions (see IER). The dipole moment value was taken from Kondo and Oka[82] and the resulting line intensities are accurate to ≈2–5%. A constant air-broadened halfwidth of 0.107 cm^{-1}/atm was assigned to the data, unchanged from previous editions of the database.

O. HOCl

The pure rotational bands of the two isotopic species of hydrogen hypochlorite, $HO^{35}Cl$ and $HO^{37}Cl$, were added to the database. The data and calculational method are given in Singbeil *et al.*[83] The chlorine hyperfine structure has been omitted in the compilation since the splittings are generally smaller than the width of lower stratospheric lines. The calculations considered values of K up to 20. An arbitrary air-broadened halfwidth of 0.06 cm^{-1}/atm was assumed for the data. The line position accuracy is transition dependent and reported in IER. In general the uncertainty is better than 0.005 cm^{-1}. The line intensities are accurate to 5%.

P. HCN

The hydrogen cyanide air-broadened halfwidths were updated from the constant value used on previous editions of the database. The air-broadened values are based on the N_2-broadening measurements of Smith *et al.*[84] The measurements give values of the halfwidths as a function of $|m|$ and range from $|m| = 1$ to 26. The relative uncertainty of the air-broadened halfwidths is estimated at 10–20% and the values are in good agreement with the results of Varghese and Hanson.[85] Beyond the range of measurements, a constant value of 0.099 cm^{-1}/atm was assumed.

Q. H_2O_2

The pure rotation band of hydrogen peroxide was added to this edition of the database. The spectral lines and method of calculation are from Helminger *et al.*[86] and additional lines and the dipole moment were measured by Cohen and Pickett.[87] Data are given for the $\tau = 1$, 2, 3, and 4 torsional states. The line positions have a transition-dependent uncertainty with the worst case being ≈0.03 cm^{-1} improving to 0.000001 cm^{-1} for many of the lines. The error is given by the first number of the IER parameter. The line intensities are accurate to ≈2–5%. Updated line parameters for the ν_6 fundamental are now available[88] but not included in the compilation. A value of 0.10 cm^{-1}/atm was assumed for the air-broadened halfwidth, close to recent experimental measurements.[89]

R. C_2H_2

A total of eight bands of acetylene are represented on HITRAN as shown in Table V. The band center frequencies for the first four bands are from Varanasi *et al.*[90]; the band center frequencies for the remaining bands are from Rinsland *et al.*[91]

The sources for the line positions and intensities are as follows. In the 12–14-μm (ν_5 fundamental) region, the results are from Varanasi *et al.*[90] These parameters are the same as those in the 1984 GEISA compilation.[5] In the 3-μm (ν_3 fundamental) region, the parameters are from the work of Rinsland *et al.*[91] The ν_3 fundamental of $H^{12}C^{13}CH$ has been added since the 1982 trace gas compilation.[4]

The air-broadened halfwidths are the experimental values measured by Devi *et al.*[92] P- and R-branch widths corresponding to the same value of $|m|$ have been averaged, except for $|m| = 1$ ($R0$ and $P1$) where experimental results indicate significant differences between the widths. Beyond the range of measurements ($|m| \geq 32$), the halfwidths have been arbitrarily extrapolated to an asymptotic value of 0.04 cm^{-1}/atm at 296 K.

The self-broadened halfwidths have been computed using a polynomial in $|m|$ expansion derived from experimental data by Varanasi *et al.*[93] Above $|m| = 25$, a constant value of 0.11 cm^{-1}/atm at 296 K has been assumed. For Q-branch lines, both the air-broadened and self-broadened widths have been calculated using the expressions for the P- and R-branch transitions.

S. Temperature Dependence of Halfwidths

The temperature dependence of the halfwidth, n, is a new parameter in this edition of the database that has applications in infrared remote sensing and accurate transmission studies.

This parameter is now being measured for many of the gases in the atmosphere. The form of the temperature dependence can be understood in terms of a specific model. Here the halfwidth in cm^{-1}/atm is

written as the product of density, velocity, and the optical cross section,

$$\gamma(T) = \rho(T) \cdot \upsilon(T) \cdot \sigma(T). \quad (7)$$

The temperature dependence of the density ($n_0 \cdot 273/T$) and velocity $(8kT/\pi\mu)^{1/2}$ are known. The optical cross section is assumed to vary in the form $\sigma(T) = T^m \cdot \sigma_0$, where σ_0 is independent of temperature. Taking the ratio of the halfwidth at two temperatures gives

$$\gamma(T_1) = \gamma(T_2) \cdot \left(\frac{T_1}{T_2}\right)^{-1/2} \cdot \left(\frac{T_1}{T_2}\right)^{m} \cdot \quad (8)$$

Setting $-n = -1/2 + m$ produces the usual formula

$$\gamma(T_1) = \gamma(T_2) \cdot \left(\frac{T_1}{T_2}\right)^{-n} \cdot \quad (9)$$

On the database the ratio of temperatures is inverted to remove the minus sign [Eq. (4)]. The temperature dependence is contained in the value of the exponent n. This model also gives the temperature dependence, m, of the optical cross section which can be useful to other studies. For molecules where there are no measured values of n available, the optical cross section is assumed temperature independent ($m = 0$) giving a temperature dependence of $n = 1/2$; this is sometimes called the classical value. The values of n used on the database are given in Table II and described below.

For water vapor, in the theoretical work of Davies and Oli,[12] three pure rotation lines and one ν_2 line were studied. The average exponent for N_2-broadening of the pure rotation lines was 0.64 and the ν_2 value was $n = 0.45$. These results have been discussed[13] and the value $n = 0.64$ was adopted for all water lines. In the future, the results of Gamache and Rothman,[94] theoretical calculations of n for some fifty water vapor transitions for both pure rotation and ν_2 bands, will be added to the H_2O lines on the database.

The temperature exponents used for carbon dioxide take into account the observed vibrational dependence of n. A value of $n = 0.75$ from the measurements of Planet *et al.*[95] is used for all bands except lines in the ν_3 band and the overtone band, $\nu_2 + \nu_3 - \nu_2$. The data for these latter bands are from Devi *et al.*[96] and have the values $n = 0.76$ and $n = 0.79$, respectively.

The temperature exponent for all ozone transitions was taken from the calculations of Gamache.[97] These calculations considered 126 rotational–vibrational transitions and yield n as a function of J and K_a. The results compared well to the few experimental measurements available. From this work an average temperature exponent of $n = 0.76$ was adopted.

The values of the temperature exponents of the air-broadened halfwidth for N_2O are transition dependent and were taken from the work of Lacome *et al.*[41] Transitions that do not have a value reported in Ref. 41 use an average value of $n = 0.75$ from Varanasi.[98]

For carbon monoxide the temperature exponent has been determined in several studies. Varanasi *et al.*[99] determined a value of $n = 0.75$. More recently Hartmann *et al.*[100] experimentally determined a value of $n = 0.69 \pm 0.02$ which agrees well with the calculations of Bonamy *et al.*[101] The value adopted for the CO lines on the database was $n = 0.69$.

Several different temperature exponents are being used for methane, reflecting the dependence of n on the symmetry species of the transition. The values from Varanasi *et al.*[58] are $n = 0.63$ for the A-species, $n = 0.75$ for the E-species, and $n = 1.0$ for all F-species. For monodeuterated methane (CH_3D) a value of $n = 0.75$ from Varanasi *et al.*[59] has been adopted. The next edition of the database will incorporate the recent work of Devi *et al.*[102] in the evaluation of the exponent.

In future versions of the database, a value of 0.968 will be adopted for the temperature exponent of NO_2, based on N_2-broadened measurements of Devi *et al.*[103]

The temperature exponents for the halfwidths of hydrogen chloride were taken from the work of Ballard *et al.*[79] and vary from a maximum of 0.88 to a minimum of 0.20. For lines that do not have a measured temperature exponent the classical value was used, $n = 0.5$.

A value of $n = 0.75$ has been assumed for the temperature dependence of the halfwidths for all lines of acetylene based on the N_2-broadened measurements of Varanasi *et al.*,[93] which were obtained at 153 and 200 K.

All other molecules on the database presently use the classical value of $n = 0.5$. As data become available for the temperature exponent they will be reviewed for addition to the HITRAN database.

III. Cross Sections: Description and Application

There are several important atmospheric molecules with significant infrared features in specific spectral regions for which no line parameters are presently available. This category includes molecules such as the chlorofluorocarbons (CFCs), for which no line parameters are available in any spectral region, and also molecules such as HNO_3, for which good line parameters are available for only some of the important spectral regions.

For such cases the current edition of the HITRAN database provides a separate file of high resolution cross sections for a first approximation simulation of their spectra. These are approximate cross sections, derived by the Lambert-Beer law from 0.02-cm^{-1} resolution room temperature laboratory absorption spectra acquired at the University of Denver,[104] as described by Massie *et al.*[105] In general, the accuracy of the data is of the order of 10–25%, but one should note that they are pressure independent and applicable for small absorptions only.

It is anticipated that some of these cross-sectional sets will be replaced by individual line parameters as they become available. However, for most heavy molecules with complex overlapping line structure (usually also with several hot bands), it will be unrealistic to expect line parameters for more than a few preselected narrow intervals. As an example, recent work[106] on the ν_6 region of CF_2Cl_2 shows that the 921–923-cm^{-1} region can be modeled satisfactorily on a line-by-line basis, but this requires over 50,000 individual lines. Thus, for wider spectral intervals of such molecules,

higher resolution (0.005 cm^{-1}) and temperature and pressure-dependent semiempirical cross sections will be required. Indeed, progress is being made toward these goals, as in the cases of the temperature-dependent cross sections of the major CF_2Cl_2 and $CFCl_3$ bands[107] and of the $ClONO_2$ bands.[108]

The cross sections σ_ν (cm^{-1}/molec·cm^{-2}) can be incorporated directly into a line-by-line calculation as additive spectral values to the infinite resolution line absorption coefficients (with proper wavenumber interpolation), before the instrument function is applied. It is also possible to simulate the spectra by generating artificial line parameters such as has been done for the chlorine nitrate ($ClONO_2$) ν_4 Q-branch.[109] In both approaches—until further information becomes available—the temperature dependence of the cross sections can be approximated by a rigid rotor, harmonic oscillator partition function with an effective rotation–vibration ground state energy.

It should be emphasized that, while the accuracy of the cross-sectional method is limited (especially for strong absorptions), omitting them in spectral regions where no line parameters are available leads to much larger errors in the interpretation of line-by-line simulations of atmospheric spectra.

Table VI summarizes the cross sections contained in file 4 on the HITRAN database. This file provides the molecule, the spectral interval, and the number of cross-sectional points in a header that appears at the beginning of data for each of the seventeen bands of the eleven heavy molecular species represented at this time. Each header contains additional information concerning the experimental conditions used at the University of Denver. The main body of the data after the header gives the cross sections at the discrete wavenumber steps determined by the spectral interval and the number of points.

IV. Concluding Remarks

This new edition of the HITRAN database represents the first major departure from the format originally established[1] by the Group on Atmospheric Transmission. This has been made necessary in part by the need and availability of molecular parameters for diverse applications. In addition, the previously separate compilations for the principal infrared telluric atmospheric absorbers and the species with lesser optical depth, are now united in one database. The overall goal in constructing the new HITRAN database has been for the database to be accessible and consistent; future editions may require additional parameters and information, but the user interface should provide a minimum of problems.

Updating is proceeding on several different aspects. As indicated in Sec. II, new data for several bands that are quite deficient on the database became available after this edition was finalized. These include new high resolution analyses[110] for water vapor in the visible region that would extend the database to ~23,000 cm^{-1}. There is also the continuing effort to improve the band intensities of carbon dioxide following the methods previously mentioned.[14,15] The latter effort is being enhanced by the attainment of better photometric accuracy for bands in the 4.3-, 14-, and 15-μm regions.[111,112] The first high resolution analysis of ozone isotopic bands[22,23] will make an immense improvement on the database. It is expected that with high temperature nitrous oxide measurements in progress[113] and methods similar to those in progress for CO_2, the parameters for N_2O will be substantially improved in the near future. As mentioned previously, the ν_2 band of nitric acid will be updated. The recent highly accurate measurements of HCl and HF intensities, broadening, and shifts by Pine *et al.*[78] and Chackerian *et al.*[80] will be incorporated. The quadrupole lines of nitrogen will also be updated.[114] It is anticipated that some of the species on the cross-sectional file, such as CF_2Cl_2, will become available for the main database. In addition, many of the new parameters compiled for the ATMOS experiment[115] will be evaluated and be placed on the next HITRAN database. The modifications outlined here represent a small fraction of the updates planned for a future edition.

A major thrust in future editions of the database will be to update halfwidths, both air- and self-broadened. The literature abounds with new data, especially for the latter parameter. Likewise, pressure shifts are now being observed and will be incorporated into the field that has been reserved for them. An effort will be made to acquire more line coupling parameters, such as for the oxygen 60-GHz lines. To include temperature dependency of the line coupling, a table with an interpolation scheme may be required. Similarly, we plan to provide the internal partition sum in tabular form for interpolating for different temperatures. Having the partition sum at 296 K will also facilitate the proper implementation of the transition probability parameter on the compilation. Hopefully, some implementation of the scheme for tagging references and criteria for the major parameters will be accomplished (this is a somewhat monumental and hazardous task).

The compilation can be obtained on a magnetic tape from the National Climatic Data Center, National Oceanic & Atmospheric Administration, Federal Building, Asheville, NC 28801.

This database is the result of cooperation and collaboration on an international scale; it would be difficult to acknowledge all those who have participated and contributed to this effort. We are deeply grateful to the spectroscopists and theoreticians who submitted their work, often prior to publication. In addition to contributions from other researchers from the authors' institutions, we would like to acknowledge the contributions from the following laboratories: Laboratoire d'Infrarouge, CNRS, France; the College of William & Mary; the Ohio State University; the Rutherford Appleton Laboratory, U.K.; Stewart Radiance Laboratory, Utah State University; the National Research Council of Canada; the National Bureau of Standards; the National Center for Atmospheric Research; and Visidyne, Inc. We would also like to express our deep appreciation to Kenneth F. Kozik of

Digital Equipment Corp. for his assistance in software management for this project. This program has been supported by the Air Force Office of Scientific Research through AFGL Task 2310G1.

References

1. R. A. McClatchey, W. S. Benedict, S. A. Clough, D. E. Burch, R. F. Calfee, K. Fox, L. S. Rothman, and J. S. Garing, "AFCRL Atmospheric Absorption Line Parameters Compilation," AFCRL-TR-0096 (AFCRL, Bedford, MA, 1973).
2. L. S. Rothman, "AFGL Atmospheric Absorption Line Parameters Compilation: 1980 Version," Appl. Opt. **20,** 791 (1981); L. S. Rothman *et al.*, "AFGL Trace Gas Compilation: 1980 Version," Appl. Opt. **20,** 1323 (1981).
3. L. S. Rothman *et al.*, "AFGL Atmospheric Absorption Line Parameters Compilation: 1982 Edition," Appl. Opt. **22,** 2247 (1983).
4. L. S. Rothman *et al.*, "AFGL Trace Gas Compilation: 1982 Version," Appl. Opt. **22,** 1616 (1983).
5. N. Husson *et al.*, "The GEISA Spectroscopic Line Parameters Data Bank in 1984," Ann. Geophys. **4,** 185 (1986).
6. R. L. Poynter and H. M. Pickett, "Submillimeter, Millimeter, and Microwave Spectral Line Catalog," Appl. Opt. **24,** 2235 (1985).
7. J. K. Messer, F. C. DeLucia, and P. Helminger, "Submillimeter Spectroscopy of the Major Isotopes of Water," J. Mol. Spectrosc. **105,** 139 (1984).
8. R. A. Toth and R. L. Poynter, "Line Positions and Line Strengths of the (010–000) and (020–010) Bands of $HD^{16}O$ and the (010–000) Band of $HD^{18}O$," in preparation.
9. J.-M. Flaud, C. Camy-Peyret, and R. A. Toth, *Selected Constants: Water Vapour Line Parameters from Microwave to Medium Infrared* (Pergamon, Oxford, 1981).
10. R. A. Toth, Jet Propulsion Laboratory; unpublished data.
11. R. R. Gamache and R. W. Davies, "Theoretical Calculations of N_2-Broadened Halfwidths of H_2O Using Quantum Fourier Transform Theory," Appl. Opt. **22,** 4013 (1983).
12. R. W. Davies and B. A. Oli, "Theoretical Calculations of H_2O Linewidths and Pressure Shifts: Comparison of the Anderson Theory with Quantum Many-Body Theory for N_2 and Air-Broadened Lines," J. Quant. Spectrosc. Radiat. Transfer **20,** 95 (1978).
13. R. W. Davies, GTE Laboratories; private communication (1980).
14. L. S. Rothman, "Infrared Energy Levels and Intensities of Carbon Dioxide. Part 3," Appl. Opt. **25,** 1795 (1986).
15. R. B. Wattson and L. S. Rothman, "Determination of Vibrational Energy Levels and Parallel Band Intensities of $^{12}C^{16}O_2$ by Direct Numerical Diagonalization," J. Mol. Spectrosc. **119,** 83 (1986).
16. L. R. Brown and R. A. Toth, "Comparison of the Frequencies of NH_3, CO_2, H_2O, N_2O, CO, and CH_4 as Infrared Calibration Standards," J. Opt. Soc. Am. B **2,** 842 (1985).
17. E. Arié, N. Lacome, P. Arcas, and A. Levy, "Oxygen- and Air-Broadened Linewidths of CO_2," Appl. Opt. **25,** 2584 (1986).
18. L. L. Strow and B. M. Gentry, "Rotational Collisional Narrowing in an Infrared CO_2 *Q* Branch Studied with a Tunable Diode Laser," J. Chem. Phys. **84,** 1149 (1986); J. Johns, National Research Council of Canada; private communication.
19. M. L. Hoke, S. A. Clough, W. Lafferty, and B. W. Olson, "Line Coupling in Carbon Dioxide," presented at the Forty-First Symposium on Molecular Spectroscopy (16–20 June 1986), paper TB9 (replacement).
20. E. W. Smith, "Absorption and Dispersion in the O_2 Microwave Spectrum at Atmospheric Pressures," J. Chem. Phys. **74,** 6658 (1981).
21. H. M. Pickett, E. A. Cohen, and J. S. Margolis, "The Infrared and Microwave Spectra of Ozone for the (0,0,0), (1,0,0) and (0,0,1) States," J. Mol. Spectrosc. **110,** 186 (1985).
22. J.-M. Flaud, C. Camy-Peyret, V. M. Devi, C. P. Rinsland, and M. A. H. Smith, "The ν_1 and ν_3 Bands of $^{16}O^{18}O^{16}O$: Line Positions and Intensities," J. Mol. Spectrosc. **118,** 334 (1986).
23. C. Camy-Peyret, J.-M. Flaud, A. Perrin, V. M. Devi, C. P. Rinsland, and M. A. H. Smith, "The Hybrid-Type Bands ν_1 and ν_3 of $^{16}O^{16}O^{18}O$: Line Positions and Intensities," J. Mol. Spectrosc. **118,** 345 (1986).
24. J.-M. Flaud, C. Camy-Peyret, V. M. Devi, C. P. Rinsland, and M. A. H. Smith, "The ν_1 and ν_3 Bands of $^{16}O_3$: Line Positions and Intensities," J. Mol. Spectrosc. (1987), in press.
25. C. P. Rinsland, V. M. Devi, J.-M. Flaud, C. Camy-Peyret, M. A. H. Smith, and G. M. Stokes, "Identification of ^{18}O-Isotopic Lines of Ozone in Infrared Ground-Based Solar Absorption Spectra," J. Geophys. Res. **90,** 10719 (1985).
26. A. Barbe, C. Secroun, A. Goldman, and J. R. Gillis, "Analysis of the $\nu_1 + \nu_2 + \nu_3$ Band of O_3," J. Mol. Spectrosc. **100,** 377 (1983).
27. C. Meunier, P. Marche, and A. Barbe, "Intensities and Air Broadening Coefficients of O_3 in the 5- and 3-μm Regions," J. Mol. Spectrosc. **95,** 271 (1982).
28. A. Goldman A. Barbe, "Line Parameters for the $\nu_1 + \nu_2 + \nu_3$ Bands of O_3," DU-Reims Collaborative Studies on Atmospheric Spectroscopy, Final Report (Oct. 1985).
29. H. M. Pickett *et al.*, "The Vibrational and Rotational Spectra of Ozone for the (0,1,0) and (0,2,0) States," J. Mol. Spectrosc. in press.
30. A. Goldman, J. R. Gillis, and A. Barbe, "Calculated Line Parameters for the $2\nu_2$ $^{16}O_3$ Band," Technical Report, Physics Department, U. Denver (1983).
31. A. Goldman, R. D. Blatherwick, F. J. Murcray, J. W. VanAllen, F. H. Murcray, and D. G. Murcray, "New Atlas of Stratospheric IR Absorption Spectra, Volume I: Line Positions and Identifications. Volume II: The Spectra," U. Denver (Sept. 1986).
32. V. M. Devi, J.-M. Flaud, C. Camy-Peyret, C. P. Rinsland, and M. A. H. Smith, "Line Positions and Intensities for the $\nu_1 + \nu_2$ and $\nu_2 + \nu_3$ Bands of $^{16}O_3$," J. Mol. Spectrosc. (1987), in press.
33. R. R. Gamache and L. S. Rothman, "Theoretical N_2-broadened Halfwidths of $^{16}O_3$," Appl. Opt. **24,** 1651 (1985).
34. R. R. Gamache and R. W. Davies, "Theoretical N_2-, O_2-, and Air-Broadened Halfwidths of $^{16}O_3$ Calculated by Quantum Fourier Transform Theory with Realistic Collision Dynamics," J. Mol. Spectrosc. **109,** 283 (1985).
35. M. A. H. Smith, K. B. Thakur, C. P. Rinsland, V. M. Devi, and D. C. Benner, "Diode Laser Measurements in the ν_1 Band of $^{16}O_3$," presented at the Forty-First Symposium on Molecular Spectroscopy, paper RF6, (16–20 June 1986); M. A. H. Smith, C. P. Rinsland, V. M. Devi, D. C. Benner, and K. B. Thakur, "Measurements of Air-Broadened and Nitrogen-Broadened Halfwidths and Shifts of Ozone Lines near 9 μm," J. Opt. Soc. Am. B (1987), submitted.
36. R. A. Toth, "Line Strengths of N_2O in the 1120–1440-cm^{-1} Region," Appl. Opt. **23,** 1825 (1984).
37. R. A. Toth, "Frequencies of N_2O in the 1100- to 1440-cm^{-1} Region," J. Opt. Soc. Am. B **3,** 1263 (1986).
38. R. A. Toth, "N_2O Vibration–Rotation Parameters Derived from Measurements in the 900–1090- and 1580–2380-cm^{-1} Regions," J. Opt. Soc. Am. B **4,** 357 (1987).
39. R. A. Toth, "Line Strengths (1100–2370 cm^{-1}) Self-Broadened Linewidths and Frequency Shifts (1800–2630 cm^{-1}) of N_2O and Isotopic Variants," in preparation.
40. W. B. Olson, A. G. Maki, and W. J. Lafferty, "Tables of N_2O Absorption Lines for the Calibration of Tunable Infrared Lasers from 522 cm^{-1} to 657 cm^{-1} and from 1115 cm^{-1} to 1340 cm^{-1}," J. Chem. Phys. Ref. Data **10,** 1065 (1981).

41. N. Lacome, A. Levy, and G. Guelachvili, "Fourier Transform Measurement of Self-, N_2-, and O_2-Broadening of N_2O Lines: Temperature Dependence of Linewidths," Appl. Opt. **23,** 425 (1984).
42. J. C. Hilico, M. Loete, and L. R. Brown, "Line Strengths of the ν_3–ν_4 Band of Methane," J. Mol. Spectrosc. **111,** 119 (1985).
43. G. Tarrago, K. N. Rao, and L. W. Pinkley, "Analysis of the ν_3 Band of $^{12}CH_3D$ at 7.6 μm," J. Mol. Spectrosc. **79,** 31 (1980).
44. G. Tarrago, Laboratoire d'Infrarouge, France; unpublished data (1980).
45. L. W. Pinkley, K. N. Rao, G. Tarrago, G. Poussigue, and M. Dang-Nhu, "Analysis of the ν_6 Band of $^{12}CH_3D$ at 8.6 μm," J. Mol. Spectrosc. **68,** 195 (1977).
46. G. Poussigue, G. Tarrago, P. Cardinet, and A. Valentin, "Absorption of Monodeuteromethane $^{12}CH_3D$ at 4.5 μm. Analysis of the Overtone Band $2\nu_6$," J. Mol. Spectrosc. **82,** 35 (1980).
47. G. Poussigue, E. Pascaud, J. P. Champion, and G. Pierre, "Rotational Analysis of Vibrational Polyads in Tetrahedral Molecules. Stimultaneous Analysis of the Pentad Energy Levels of $^{12}CH_4$," J. Mol. Spectrosc. **93,** 351 (1982).
48. G. Pierre, J. P. Champion, G. Guelachvili, E. Pascaud, and G. Poussigue, "Rotational Analysis of Vibrational Polyads in Tetrahedral Molecules: Line Parameters of the Infrared Spectrum of $^{12}CH_4$ in the Range 2250–3260 cm^{-1}: Theory Versus Experiment," J. Mol. Spectrosc. **102,** 344 (1983).
49. R. A. Toth, L. R. Brown, R. H. Hunt, and L. S. Rothman, "Line Parameters of Methane from 2385 to 3200 cm^{-1}," Appl. Opt. **20,** 932 (1981).
50. L. R. Brown, Jet Propulsion Laboratory; unpublished data.
51. D. J. E. Knight, G. J. Edwards, P. R. Pearce, and N. R. Cross, "Measurement of the Frequency of the 3.39-μm Methane-Stabilized Laser to ± 3 Parts in 10^{11}," IEEE Trans. Instrum. Meas. **IM-29,** 257 (1980).
52. L. R. Brown and L. S. Rothman, "Methane Line Parameters for the 2.3-μm Region," Appl. Opt. **21,** 2425 (1982).
53. L. R. Brown, "Laboratory Spectroscopy to Support Remote Sensing of Planetary Atmospheres: Experimental Line Parameters of Methane at 2.55 μm," in *Abstracts, Ninth Colloquium on High Resolution Molecular Spectroscopy*, Riccione, Italy (Sept. 1985).
54. C. R. Pollock, F. R. Petersen, D. A. Jennings, J. S. Wells, and A. G. Maki, "Absolute Frequency Measurements of the 2–0 Band of CO at 2.3 μm; Calibration Standard Frequencies from High Resolution Color Center Laser Spectroscopy," J. Mol. Spectrosc. **99,** 357 (1983).
55. J. S. Margolis, "Line Strength Measurements of the $2\nu_3$ Band of Methane," J. Quant. Spectrosc. Radiat. Transfer **13,** 1097 (1973).
56. K. Fox, G. W. Halsey, and D. E. Jennings, "High Resolution Spectrum and Analysis of $2\nu_3$ of $^{13}CH_4$ at 1.67 μm," J. Mol. Spectrosc. **83,** 213 (1980).
57. G. D. T. Tejwani and K. Fox, "Calculated Linewidths for CH_4 Broadened by N_2 and O_2," J. Chem. Phys. **60,** 2021 (1974); G. D. T. Tejwani and K. Fox, "Calculated Self- and Foreign-Gas Broadened Linewidths for CH_3D," J. Chem. Phys. **61,** 759 (1974).
58. P. Varanasi, L. P. Giver, and F. P. J. Valero, "Thermal Infrared Lines of Methane Broadened by Nitrogen at Low Temperatures," J. Quant. Spectrosc. Radiat. Transfer **30,** 481 (1983).
59. P. Varanasi, L. P. Giver, and F. P. J. Valero, "A Laboratory Study of the 8.65 μm Fundamental of $^{12}CH_3D$ at Temperatures Relevant to Titan's Atmosphere," J. Quant. Spectrosc. Radiat. Transfer **30,** 517 (1983).
60. V. M. Devi, C. P. Rinsland, M. A. H. Smith, and D. C. Benner, "Measurements of $^{12}CH_4$ ν_4 Band Halfwidths Using a Tunable Diode Laser System and a Fourier Transform Spectrometer," Appl. Opt. **24,** 2788 (1985).
61. V. M. Devi, C. P. Rinsland, M. A. H. Smith, and D. C. Benner, "Tunable Diode Laser Measurements of Widths of Air- and Nitrogen-Broadened Lines in the ν_4 Band of $^{13}CH_4$," Appl. Opt. **24,** 3321 (1985).
62. F. J. Lovas, "Microwave Spectral Tables II. Triatomic Molecules," J. Phys. Chem. Ref. Data **7,** 1445 (1978).
63. M. Carlotti, G. DiLonardo, L. Fusina, B. Carli, and F. Mencaraglia, "The Submillimeter-Wave Spectrum and Spectroscopic Constants of SO_2 in the Ground State," J. Mol. Spectrosc. **106,** 235 (1984).
64. D. Patel, D. Margolese, and T. R. Dyke, "Electric Dipole Moment of SO_2 in Ground and Excited States," J. Chem. Phys. **70,** 2740 (1979).
65. C. Camy-Peyret, J.-M. Flaud, A. Perrin, and K. N. Rao, "Improved Line Parameters for the ν_3 and $\nu_2 + \nu_3 - \nu_2$ Bands of $^{14}N^{16}O_2$," J. Mol. Spectrosc. **95,** 72 (1982).
66. V. M. Devi *et al.*, "Tunable Diode Laser Spectroscopy of NO_2 at 6.2 μm," J. Mol. Spectrosc. **93,** 179 (1982).
67. A. Perrin, J.-M. Flaud, and C. Camy-Peyret, "Calculated Line Positions and Intensities for the $\nu_1 + \nu_3$ and $\nu_1 + \nu_2 + \nu_3 - \nu_2$ Bands of $^{14}N^{16}O_2$," Infrared Phys. **22,** 343 (1982).
68. R. A. Toth and R. H. Hunt, "Line Strengths, Spin-Splittings, and Forbidden Transitions in the (101) Band of $^{14}N^{16}O_2$," J. Mol. Spectrosc. **79,** 182 (1980).
69. J.-M. Flaud, C. Camy-Peyret, V. Malathy Devi, P. P. Das, and K. Narahari Rao, "Diode Laser Spectra of the ν_2 Band of $^{14}N^{16}O_2$: The (010) State of NO_2," J. Mol. Spectrosc. **84,** 234 (1980).
70. V. M. Devi, P. P. Das, A. Bano, K. N. Rao, J.-M. Flaud, C. Camy-Peyret, and J.-P. Chevillard, "Diode Laser Measurements of Intensities, N_2-Broadening, and Self-Broadening Coefficients of Lines of the ν_2 Band of $^{14}N^{16}O_2$," J. Mol. Spectrosc. **88,** 251 (1981).
71. W. C. Bowman and F. C. DeLucia, "The Millimeter and Submillimeter Spectrum of NO_2: A Study of Electronic Effects in a Nonsinglet Light Asymmetric Rotor," J. Chem. Phys. **77,** 92 (1982).
72. R. L. Poynter and J. S. Margolis, "The ν_2 Spectrum of NH_3," Mol. Phys. **51,** 393 (1984).
73. A. G. Maki, W. B. Olson, A. Fayt, J. S. Wells, and A. Goldman, "High Resolution Measurements and Analysis of the ν_2, ν_3, ν_4, ν_5, and $2\nu_9$ Bands of Nitric Acid," presented at *Forty-First Symposium on Molecular Spectroscopy*, Ohio State U. (1986), paper TE8.
74. A. Goldman, J. R. Gillis, C. P. Rinsland, F. J. Murcray, and D. G. Murcray, "Stratospheric HNO_3 Quantification from Line-by-Line Nonlinear Least-Squares Analysis of High-Resolution Balloon-Borne Solar Absorption Spectra in the 870-cm^{-1} Region," Appl. Opt. **23,** 3252 (1984); D. G. Murcray, F. H. Murcray, F. J. Murcray, and G. Vanasse, "Measurements of Atmospheric Emission at High Spectral Resolution," J. Meteorol. Soc. Jpn. **63,** 320 (1985).
75. A. Goldman, U. Denver, unpublished data.
76. A. Maki, "High Resolution Measurements of the ν_2 Band of HNO_3 and the ν_3 Band of Trans-HONO," J. Mol. Spectrosc. **00,** 000 (198X), in press.
77. R. E. Thompson, J. H. Park, M. A. H. Smith, G. A. Harvey, and J. M. Russell III, "Nitrogen-Broadened Halfwidths of HF Lines in the 1–0 Band," J. Mol. Spectrosc. **106,** 251 (1984).
78. A. S. Pine, A. Fried, and J. W. Elkins, "Spectral Intensities in the Fundamental Bands of HF and HCl," J. Mol. Spectrosc. **109,** 30 (1985); A. S. Pine and J. P. Looney, "N_2 and Air Broadening in the Fundamental Bands of HF and HCl," J. Mol. Spectrosc. **122,** 41 (1987); A. S. Pine and A. Fried, "Self-Broadening in the Fundamental Bands of HF and HCl," J. Mol. Spectrosc. **114,** 148 (1985).

79. J. Ballard, W. B. Johnston, P. H. Moffat, and D. T. Llewellyn-Jones, "Experimental Determination of the Temperature Dependence of Nitrogen Broadened Line Widths in the 1–0 Band of HCl," J. Quant. Spectrosc. Radiat. Transfer **33,** 365 (1985).
80. C. Chackerian, Jr., D. Goorvitch, and L. P. Giver, "HCl Vibrational Fundamental Band: Line Intensities and Temperature Dependence of Self-Broadening Coefficients," J. Mol. Spectrosc. **113,** 373 (1985).
81. W. H. Kirchhoff, "On the Calculation and Interpretation of Centrifugal Distortion Constants: A Statistical Basis for Model Testing: The Calculation of the Force Field," J. Mol. Spectrosc. **41,** 333 (1972).
82. K. Kondo and T. Oka, "Stark-Zeeman Effects on Asymmetric Top Molecules. Formaldehyde H_2CO," J. Phys. Soc. Jpn. **15,** 307 (1960).
83. H. E. G. Singbeil *et al.*, "The Microwave and Millimeter Wave Spectra of Hypochlorous Acid," J. Mol. Spectrosc. **103,** 466 (1984).
84. M. A. H. Smith, G. A. Harvey, G. L. Pellett, A. Goldman, and D. J. Richardson, "Measurements of the HCN ν_3 Band Broadened by N_2," J. Mol. Spectrosc. **105,** 105 (1984).
85. P. L. Varghese and R. K. Hanson, "Tunable Diode Laser Measurements of Spectral Parameters of HCN at Room Temperature," J. Quant. Spectrosc. Radiat. Transfer **31,** 545 (1984).
86. P. Helminger, W. C. Bowman, and F. C. DeLucia, "A Study of the Rotational-Torsional Spectrum of Hydrogen Peroxide between 80 and 700 GHz," J. Mol. Spectrosc. **85,** 120 (1981).
87. E. A. Cohen and H. Pickett, "The Dipole Moment of Hydrogen Peroxide," J. Mol. Spectrosc. **87,** 582 (1981).
88. J. J. Hillman, D. E. Jennings, W. B. Olson, and A. Goldman, "High-Resolution Infrared Spectrum of Hydrogen Peroxide: The ν_6 Fundamental Band," J. Mol. Spectrosc. **117,** 46 (1986).
89. V. M. Devi, C. P. Rinsland, M. A. H. Smith, D. C. Benner, and B. Fridovich, "Tunable Diode Laser Measurements of Air-Broadened Linewidths in the ν_6 Band of H_2O_2," Appl. Opt. **25,** 1844 (1986).
90. P. Varanasi, L. P. Giver, and F. P. J. Valero, "Infrared Absorption by Acetylene in the 12–14 μm Region at Low Temperatures," J. Quant. Spectrosc. Radiat. Transfer **30,** 497 (1983).
91. C. P. Rinsland, A. Baldacci, and K. N. Rao, "Acetylene Bands Observed in Carbon Stars: A Laboratory Study and an Illustrative Example of Its Application to IRC+10216," Astrophys. J. Suppl. **49,** 487 (1982).
92. V. M. Devi, D. C. Benner, C. P. Rinsland, M. A. H. Smith, and B. D. Sidney, "Tunable Diode Laser Measurements of N_2- and Air-Broadened Halfwidths: Lines in the $(\nu_4 + \nu_5)^0$ Band of $^{12}C_2H_2$ Near 7.4 μm," J. Mol. Spectrosc. **114,** 49 (1985).
93. P. Varanasi, L. P. Giver, and F. P. J. Valero, "Measurements of Nitrogen-Broadened Line Widths of Acetylene at Low Temperatures," J. Quant. Spectrosc. Radiat. Transfer **30,** 505 (1983).
94. R. R. Gamache and L. S. Rothman, "Temperature Dependence of N_2-Broadened Halfwidths of Water Vapor: the Pure Rotation and ν_2 Bands," J. Mol. Spectrosc. (1987), submitted.
95. W. G. Planet, G. L. Tettemer, and J. S. Knoll, "Temperature Dependence of Intensities and Widths of N_2-Broadened Lines in the 15 μm CO_2 Band from Tunable Laser Measurements," J. Quant. Spectrosc. Radiat. Transfer **20,** 547 (1978); W. G. Planet and G. L. Tettemer, "Temperature Dependent Intensities and Widths of N_2-Broadened CO_2 Lines at 15 μm Band from Tunable Laser Measurements," J. Quant. Spectrosc. Radiat. Transfer **22,** 345 (1979); G. L. Tettemer and W. G. Planet, "Intensities and Pressure-Broadened Widths of CO_2 R-Branch Lines at 15 μm from Tunable Laser Measurements," J. Quant. Spectrosc. Radiat. Transfer **24,** 343 (1980).
96. V. M. Devi, B. Fridovich, G. D. Jones, and D. G. S. Snyder, "Diode Laser Measurements of Strengths, Half-Widths, and Temperature Dependence of Half-Widths for CO_2 Spectral Lines Near 4.2 μm," J. Mol. Spectrosc. **105,** 61 (1984).
97. R. R. Gamache, "Temperature Dependence of N_2-Broadened Halfwidths of Ozone," J. Mol. Spectrosc. **114,** 31 (1985).
98. P. Varanasi, SUNY-Stony Brook; private communication.
99. P. Varanasi, "Measurement of Line Widths of CO of Planetary Interest at Low Temperatures," J. Quant. Spectrosc. Radiat. Transfer **15,** 191 (1975); P. Varanasi and S. Sarangi, "Measurements of Intensities and Nitrogen-Broadened Linewidths in the CO Fundamental at Low Temperatures," J. Quant. Spectrosc. Radiat. Transfer **15,** 473 (1975).
100. J. M. Hartmann, M. Y. Perrin, J. Taine, and L. Rosenmann, "Diode Laser Measurements and Calculations of CO 1–0 $P(4)$ Line-Broadening in the 294–765K Temperature Range," J. Mol. Spectrosc., submitted.
101. J. Bonamy, D. Robert, and C. Boulet, "Simplified Models for the Temperature Dependence of Linewidths at Elevated Temperatures and Applications to CO Broadened by Ar and N_2," J. Quant. Spectrosc. Radiat. Transfer **31,** 23 (1984).
102. V. M. Devi, B. Fridovich, G. D. Jones, and D. G. S. Snyder, "Strengths and Lorentz Broadening Coefficients for Spectral Lines in the ν_3 and $\nu_2 + \nu_4$ Bands of $^{12}CH_4$ and $^{13}CH_4$," J. Mol. Spectrosc. **97,** 333 (1983).
103. V. M. Devi, B. Fridovich, G. D. Jones, D. G. S. Snyder, and A. C. Neuendorffer, "Temperature Dependence of the Widths of N_2-Broadened Lines of the ν_3 Band of $^{14}N^{16}O_2$," Appl. Opt. **21,** 1537 (1982).
104. D. G. Murcray, F. J. Murcray, A. Goldman, F. S. Bonomo, and R. D. Blatherwick, "High Resolution Infrared Laboratory Spectra," U. Denver, Physics Department (Apr. 1984).
105. S. T. Massie, A. Goldman, D. G. Murcray, and J. C. Gille, "Approximate Absorption Cross Sections of F12, F11, $ClONO_2$, N_2O_5, HNO_3, CCl_4, CF_4, F21, F113, F114, and HNO_4," Appl. Opt. **24,** 3426 (1985).
106. A. Goldman and C. Deroche, "Line Parameters for F12 in the 920 cm^{-1} Region," U. Denver, Physics Department (July 1986).
107. J. W. Elkins, R. L. Sams, and J. Wen, "Measurements of the Temperature Dependence on the Infrared Band Strengths and Shapes for Halocarbons F-11 and F-12," Natl. Bur. Stand. U.S. Report 553-K-86 (1986).
108. V. G. Kunde *et al.*, "Atmospheric Infrared Emission of $ClONO_2$ Observed by a Balloon-Borne Fourier Spectrometer," AGU Fall Meeting (1986).
109. C. P. Rinsland *et al.*, "Tentative Identification of the 780-cm^{-1} ν_4 Band Q Branch of Chlorine Nitrate in High-Resolution Solar Absorption Spectra of the Stratosphere," J. Geophys. Res. **90,** 7931 (1985).
110. J.-Y. Mandin, J.-P. Chevillard, C. Camy-Peyret, J.-M. Flaud, and J. W. Brault, "The High-Resolution Spectrum of Water Vapor between 13200 and 16500 cm^{-1}," J. Mol. Spectrosc. **116,** 167 (1986); C. Camy-Peyret *et al.*, "The High Resolution Spectrum of Water Vapor Between 16500 and 25250 cm^{-1}," J. Mol. Spectrosc. **113,** 208 (1985).
111. J. Johns, National Research Council of Canada; private communication.
112. V. Dana, U. Pierre et Marie Curie, France; private communication.
113. M. P. Esplin, Stewart Radiance Laboratory; private communication.
114. D. Reuter, D. E. Jennings, and J. W. Brault, "The $v = 1 \leftarrow 0$ Quadrupole Spectrum of N_2," J. Mol. Spectrosc. **115,** 294 (1986).
115. L. R. Brown, C. B. Farmer, C. P. Rinsland, and R. A. Toth, "Molecular Line Parameters for the Atmospheric Trace Molecule Spectroscopy (ATMOS) Experiment," submitted to Appl. Opt., 1987.